

# A sensitive survey for water maser emission towards Bok globules using the Robledo 70m antenna

José F. Gómez<sup>1</sup>, Itziar de Gregorio-Monsalvo<sup>2</sup>, Olga Suárez<sup>2</sup>, Thomas B. H. Kuiper<sup>3</sup>

## ABSTRACT

We report the most sensitive water maser survey towards Bok globules to date, using NASA's 70m antenna in Robledo de Chavela (Spain). We observed 207 positions within the Clemens & Barvainis (1988) catalog with a higher probability of harboring a young star, using as selection criteria the presence of radio continuum emission (from submillimeter to centimeter wavelengths), geometrical centers of molecular outflows, peaks in maps of high-density gas tracers ( $\text{NH}_3$  or CS), and IRAS point sources. We have obtained 7 maser detections, 6 of which (in CB 34, CB 54, CB 65, CB 101, CB 199, and CB 232) are reported for the first time here. Most of the water masers we detected are likely to be associated with young stellar objects (YSOs), except for CB 101 (probably an evolved object) and CB 65 (uncertain nature). The water maser in CB 199 shows a relatively high shift ( $\simeq 30 \text{ km s}^{-1}$ ) of its velocity centroid with respect to the cloud velocity, which is unusual for low-mass YSOs. We speculate that high-velocity masers in this kind of object could be related with episodes of energetic mass-loss in close binaries. Alternatively, the maser in CB 199 could be pumped by a protoplanetary or a young planetary nebula. CB 232 is the smallest Bok globule ( $\simeq 0.6 \text{ pc}$ ) known to be associated with water maser emission, although it would be superseded by the cases of CB 65 ( $\simeq 0.3 \text{ pc}$ ) and CB 199 ( $\simeq 0.5 \text{ pc}$ ) if their association with YSOs is confirmed. All our selection criteria have statistically compatible detection rates, except for IRAS sources, which tend to be a somewhat worse predictor for the presence of maser emission.

*Subject headings:* stars: formation — stars: pre-main sequence — ISM: globules — masers — radio lines: ISM

---

<sup>1</sup>Instituto de Astrofísica de Andalucía, CSIC, Apartado 3004, E-18080 Granada, Spain; e-mail: jfg@iaa.es

<sup>2</sup>Laboratorio de Astrofísica Espacial y Física Fundamental, INTA, Apartado 50727, E-28080 Madrid, Spain; e-mail: itziar@laeff.esa.es; olga@laeff.esa.es

<sup>3</sup>Jet Propulsion Laboratory, California Institute of Technology, 4800 Oak Grove Dr, Pasadena, CA 91109 USA

## 1. Introduction

Bok globules (Bok & Reilly 1947) are small (projected size  $\lesssim 20'$ ), isolated, and relatively simple molecular clouds, with typical masses of  $\simeq 5 - 50 M_{\odot}$  (Martin & Barrett 1978; Clemens, Yun, & Heyer 1991). These globules are usually identified and cataloged as dark patches in optical images (e.g., Clemens & Barvainis 1988, hereafter CB). The reference catalogs of Bok globules compiled by CB and Bourke, Hyland, & Robinson (1995a, hereafter BHR) in the north and south hemispheres, respectively, focused on the group of smaller Bok globules, using a size of  $< 10'$  as a selection criterion. Under the assumption that they are nearby clouds ( $d \lesssim 500$  pc), as suggested by the small number of foreground stars, the globules in the CB and BHR catalogs would in general have linear sizes  $\lesssim 1$  pc.

Some Bok globules are sites of low- and intermediate-mass star formation (e.g., Yun & Clemens 1991, 1992; Reipurth, Heathcote, & Vrba 1992). Since they are identified from optical images, without any characterization of their possible star-forming activity, catalogs of Bok globules may span a wide range of evolutionary stages, from quiescent dark cores to clusters of Herbig Ae/Be or T-Tauri stars. Therefore, systematic studies of these globules are potentially useful to study the evolution of phenomena related to star formation, like collapse, fragmentation, mass-loss, or formation of protoplanetary disks. Moreover, being small and relatively simple molecular clouds, one can study these phenomena with a lower chance of contamination from multiple generations of young stellar objects (YSOs) within the same region. For these reasons, they are interesting laboratories in the study of the star-formation processes and its evolution.

Another important reason to study star formation in Bok globules is that field stars in the solar neighborhood, and the Sun itself, may have formed in this kind of cloud. Moreover, some T Tauri stars apparently not related to known molecular clouds, may have originated in Bok globules which have dispersed, leaving isolated pre-main-sequence objects (Launhardt & Henning 1997).

An important phenomenon related to star formation is the occurrence of water maser emission at 22 GHz. This emission is a powerful tool to study the morphology and kinematics of the environment of YSOs at high angular and spectral resolution (Torrelles et al. 2002; Claussen et al. 2005). The physical conditions needed for maser excitation can be reached in both the inner parts of circumstellar disks surrounding the YSOs and in shocked gas related to winds. This dichotomy has been suggested to be an evolutionary effect by Torrelles et al. (1997, 1998), in which masers may trace bound motions (e.g., disks) in the youngest protostars, and outflows in more evolved objects.

Although water masers are more intense and widespread in high-mass star forming re-

gions, they are also present around low-mass YSOs (Wilking & Claussen 1987; Terebey, Vogel, & Myers 1992). In the case of low-mass star formation, there seems to be an evolutionary trend, with water masers tracing the youngest YSOs, i.e., Class 0 protostars. In their survey of water maser emission towards low-mass YSOs, Furuya et al. (2001) obtained a detection rate of 40% on Class 0 sources, 4% on Class I, and 0% on Class II.

Since there are several evolutionary aspects related to water maser emission, it is interesting to study this emission in Bok globules, where we can find YSOs in different evolutionary stages. However, there are very few studies of water masers towards Bok globules. Only Scappini, Caselli, & Palumbo (1991) conducted a search for water masers specifically in Bok globules. These authors observed 80 globules, and obtained a detection towards CB 3 (LBN 594), with a peak flux density of  $\simeq 77.6$  Jy. However, their detection threshold ( $\sim 4.4 - 15.7$  Jy) would miss a high fraction of masers around low-mass YSOs.

Other surveys included among their targets some objects within the globules in the CB catalog (Felli, Palagi, & Tofani 1992; Palla & Prusti 1993; Wouterloot, Brand, & Fiegle 1993; Persi, Palagi, & Felli 1994; Codella et al. 1995). To our knowledge, only three Bok globules of the CB catalog have been reported to harbor a water maser: the mentioned one in CB 3 (Scappini et al. 1991), a detection of  $\simeq 1 - 2$  Jy towards the Herbig Be star HD 250550 in CB 39 (Schwartz & Buhl 1975), and another one of  $\simeq 7.5$  Jy in CB 205 (LDN 810) obtained by Neckel et al. (1985). We are not aware of any water masers in the southern Bok globules of the BHR catalog. However, all these three globules (CB 3, CB 39, and CB 205) are somewhat different from most of the clouds in the CB catalog, since they are located at distances  $\geq 1$  kpc, and thus are larger and more massive than the globules that CB intended to compile.

In this paper, we present the most extensive and sensitive survey of water masers in Bok globules to date. We have searched for this emission towards the positions within the globules in the CB catalog with the highest probability of harboring a YSO (see Sec. 3). This survey aims to be nearly complete for possible star-forming regions in Bok globules north of declination  $\simeq -36^\circ$ , to study the conditions and characteristics of maser emission in these isolated globules. This work is complemented by high-resolution interferometric studies of the detections in this survey, to accurately determine their spatial and velocity distribution, and to pinpoint their exciting source (de Gregorio-Monsalvo et al. 2006, hereafter DG06). The present paper is structured as follows: In Sec. 2 we describe the technical details of the observations, in Sec. 3 we explain the criteria used to select the target sources, and we present our results in Sec. 4, which are further discussed in Sec. 5. We summarize our conclusions in Sec. 6.

## 2. Observations

We observed the  $6_{16} \rightarrow 5_{23}$  transition of the water molecule (rest frequency 22235.080 MHz), using the NASA 70-m antenna (DSS-63) at Robledo de Chavela (Spain). The 1.3 cm receiver of this antenna was a cooled high-electron-mobility transistor (HEMT). Water maser observations were carried out using three different backends depending on the observing dates: From 2002 March 13 to 2002 April 10, we used a 4096-channel spectrometer covering a bandwidth of 400 MHz ( $\simeq 5398 \text{ km s}^{-1}$ ), which provided a velocity resolution of  $\simeq 1.3 \text{ km s}^{-1}$ . From 2002 April 14 to 2003 July 18, we used a 256-channel spectrometer, covering a bandwidth of 10 MHz, which provided a velocity resolution of  $\simeq 0.5 \text{ km s}^{-1}$ . From 2004 July 6 to 2005 October 16, we used a 384-channel spectrometer, covering a bandwidth of 16 MHz ( $\simeq 216 \text{ km s}^{-1}$  with  $\simeq 0.6 \text{ km s}^{-1}$  resolution). At this frequency, the half-power beamwidth of the telescope is  $\simeq 41''$ . Spectra were taken in position-switching mode with the 4096- and 384-channel spectrometers, and in frequency switching mode, with a switch of 5 MHz, when using the 256-channel one, thus providing in the latter case an effective velocity coverage of  $\simeq 202 \text{ km s}^{-1}$  (15 MHz) centered at the  $V_{\text{LSR}}$  of each source. Only left circular polarization was processed. System temperatures ranged between 45 and 135 K, and the total integration time was typically 20 min per source in frequency-switching mode and 30 min (on+off) in position-switching mode. The rms pointing accuracy was better than  $10''$ . The data reduction was performed using the CLASS package, which is part of the GILDAS software.

## 3. Source Sample. Selection criteria

The target positions in our survey are those within the Bok globules cataloged by CB that show indications of possible star formation, or with higher probability of harboring a YSO. We used four selection criteria for those targets:

1. Radio continuum sources (submillimeter to centimeter wavelengths).

Low-mass stars undergoing mass-loss can show radio continuum emission from ionized winds (Anglada et al. 1992), which at cm wavelengths is not likely to be contaminated by dust emission from envelopes and disks. For the mm and submm emission, the youngest protostars (deeply embedded class 0 sources) show prominent emission at those wavelengths (André, Ward-Thompson, & Barsony 1993; Saraceno et al. 1996). The radio continuum sources were taken mainly from Anglada et al. (1992, 1998), Yun et al. (1996), and Moreira et al. (1999) at cm wavelengths, Launhardt & Henning (1997) at mm, and Launhardt, Ward-Thompson, & Henning (1997), Huard, Sandell, & Wein-

traub (1999), Huard, Weintraub, & Sandell (2000), and Visser, Richer, & Chandler (2002) at submm ones. We selected those sources located within the optical boundaries of the cloud and which were not suspected to be extragalactic objects due to their negative spectral indices (see e.g., Anglada et al. 1998).

2. Center of molecular outflows.

Molecular outflows driven by low-mass YSOs are specially powerful during the earlier evolutionary phases (Bontemps et al. 1996), which in their turn, are more likely to show water maser emission (Furuya et al. 2001). We have chosen the position of the geometrical center of the outflow (i.e. between the red- and blue shifted lobes), since we expect the driving source of the outflow to be near that position. In the case of outflows with only one lobe, we selected the position of the proposed powering source. Most molecular outflows known in Bok globules of the CB catalog have been reported by Yun & Clemens (1992, 1994a).

3. Peak of high-density molecular gas tracers.

YSOs form in the densest part of molecular clouds. The maxima in maps of high-density gas tracers like  $\text{NH}_3$  have been found to pinpoint the location of the driving sources of molecular outflows (Anglada et al. 1989; Gómez et al. 1994). For this survey we have used the peaks of  $\text{NH}_3$  maps compiled by Jijina et al. (1999), most of them observed by Lemme et al. (1996) in these globules, and peaks of CS maps published by Launhardt et al. (1998).

4. IRAS sources.

Many globules have been scarcely studied, if at all, so the previous observational signs of possible star formation are not always available. Therefore, we have also used the position of IRAS sources as possible locations of YSOs. We considered as target positions all IRAS sources listed by CB as associated with the globules in their catalog. Most of these IRAS sources show rising IRAS fluxes at longer wavelengths, which is expected for class 0 and class I objects (Wilking et al. 1989; André et al. 1993), but our search was not restricted based on their far infrared spectra.

These criteria are ordered by decreasing preference given to the observations of sources selected by each of them. After compiling the initial set of target positions (all located north of  $\delta = -36^\circ$ ) we dropped from the list most sources lying within a distance of  $\sim 21''$  from another source with equal or higher preference, since they would be within the beam of Robledo radio telescope, although we observed some positions that would have been left out by this proximity filter, specially for the ones that would fall closer to the edge of the telescope beam. With these selection criteria, the previously reported masers in CB 39 and

CB 205 are within the beam of one of the positions in our survey (see notes to Table 1). This is not the case for the maser reported in CB 3 by (Scappini et al. 1991), but DG06 found a more accurate position with interferometric data, which lies  $5''$  from the position of CB3-mm, a source that is included in our target list. Therefore, we see that our selection criteria seem appropriate to locate water maser emission that may exist in Bok globules of the CB catalog.

Using the final list of target sources, we searched for water masers around all radio-continuum sources, centers of outflows, and peak of high-density tracers, with a total of 100 observed positions. In addition to that, we also observed 107 IRAS sources with no known nearby source falling into the other three categories. The observed sources are shown in Table 1. Note that our survey includes, in many cases, more than one target position within the same globule. A total of 103 globules were covered by our observations.

Considering the sources lying within a distance of  $\sim 21''$  from each observed position, and therefore, which fell within the telescope beam for at least one of the observations, our survey covered 34 centimeter sources, 20 millimeter sources, 30 submillimeter sources, 16 centers of outflows, 16 peaks of CS maps, 18 peaks of  $\text{NH}_3$  maps, and 132 IRAS sources.

## 4. Results

### 4.1. Survey results

Tables 2 and 3 show the result of our survey of water maser emission in Bok globules. We have obtained 7 detections (Table 2), 6 of which (the ones in CB 34, CB 54, CB 65, CB 101, CB 199, and CB 232) are reported for the first time here. Of the previously known masers, only CB3-mm was detected by us. We did not detect the masers in either CB 39 or CB 205. In Figs. 1 to 7 we show the spectra of the detected masers.

With these detections, we have increased the number of sources in Bok globules known to emit water maser emission from 3 to 9. However, we note that some of the new detections are not likely to be related to their respective globules, and they could be background or foreground objects projected against the clouds (see Sec. 4.2). The ones which are most likely to be associated with YSOs in these globules are the masers in CB 34, CB 54, and CB 232 (and probably CB 199).

With respect to our selection criteria, considering the sources that fall within the beam of the telescope of a position with water maser detected, we have detected water maser emission around 2 centimeter sources (6%), 2 millimeter sources (10%), 4 submillimeter

sources (14%), 3 centers of molecular outflows (19%), 3 peaks of CS (17%), no peak of  $\text{NH}_3$  (0%), and 5 IRAS sources (4%), 2 of them without association with any of the other criteria (2%).

## 4.2. Detections: individual sources

### 4.2.1. CB 3 (CB3-mm)

CB 3 is located at a distance of  $\simeq 2.5$  kpc (Launhardt & Henning 1997). This large distance (and thus, large physical size,  $\simeq 4.5$  pc, see CB), and the presence of intermediate-mass star formation (it hosts a source of  $L_{\text{bol}} \simeq 930 M_{\odot}$ ; Launhardt et al. 1997) distinguish it from the rest of the globules in the CB catalog.

We detected water maser emission towards the millimeter source CB3-mm detected by Launhardt & Henning (1997). This source is believed to be the powering source of a powerful bipolar molecular outflow (Yun & Clemens 1992, 1994a; Codella & Bachiller 1999). The maser probably corresponds to the one detected by Scappini et al. (1991), although they reported a position  $\sim 1'$  from CB3-mm. We took spectra towards their position, but we did not detect any emission ( $3\sigma$  upper limit of 0.5 Jy on 2004 August 19, between  $V_{\text{LSR}} = -146.2$  and  $69.5 \text{ km s}^{-1}$ ), which is compatible with beam response if the emission is actually related with CB3-mm. Within the beam of the Robledo telescope from CB3-mm, there is also submillimeter emission (Launhardt et al. 1997; Huard et al. 2000), the peak of a CS map (Launhardt et al. 1998), and the source IRAS 00259+5625 (Table 1).

The maser emission is relatively strong (10 – 20 Jy), and shows variations of a factor of  $\sim 2$  (Table 3). The spectra are very rich in maser components at different velocities (Fig. 1), with variations in the velocity distribution and in the ratio between different components. The data taken in 2004 show maser emission over a wider range of velocities (from  $-85$  to  $-10 \text{ km s}^{-1}$ ), while those taken in 2005 do not show emission more blueshifted than  $-60 \text{ km s}^{-1}$ . The centroid velocity of the maser emission ( $V_{\text{LSR}} = -37.5$  to  $-52.8 \text{ km s}^{-1}$ , depending on the observing date) is within  $15 \text{ km s}^{-1}$  from the cloud velocity ( $V_{\text{LSR}} \simeq -38.3 \text{ km s}^{-1}$ , CB).

The geometry of  $\text{H}_2$  knots suggest that CB3-mm is ejecting a precessing jet (Massi, Codella, & Brand 2004). Interferometric observations of the water maser emission are also compatible with this suggestion (DG06).

Given the large number of different velocity components, and their time variation, it would be interesting to carry out an interferometric monitoring of this source, to trace the

spatial distribution and proper motions of these different components, to test the proposed scenario of a precessing jet, and to ascertain whether the maser variability is related with the presence of episodic mass-loss phenomena.

#### 4.2.2. CB 34 ([HSW99] CB 34 SMM 3/SMM 4)

CB 34 is a globule with multiple star formation (Alves & Yun 1995), located at 1.5 kpc (Launhardt & Henning 1997). We detected water maser emission towards the submillimeter source CB 34 SMM 3 (Huard et al. 2000). The maser emission was detected in August 2003, with two main components (at  $\simeq 1$  and  $8 \text{ km s}^{-1}$ , respectively) close to the cloud velocity ( $V_{\text{LSR}} \simeq 0.7 \text{ km s}^{-1}$ , CB). Several months later, the emission dropped below the detection threshold of the telescope.

In the vicinity of CB 34 SMM 3 there are several Herbig-Haro objects (HH 290N1, HH 290N2, HH290S, and HH291) and  $\text{H}_2$  knots, all forming at least three highly collimated jets in different directions (Moreira & Yun 1995; Khanzadyan et al. 2002). Within the Robledo beam from CB 34 SMM 3 also lies the submillimeter source CB 34 SMM 4 (Huard et al. 2000), and the geometrical center of the bipolar outflow reported by Yun & Clemens (1992), oriented NE-SW, although higher-resolution observations (Khanzadyan et al. 2002) seem to locate its center closer to the position of CB 34 SMM 1. Although CB 34 SMM 4 was not in our original list of targets, given that it was within the beam when observing at CB 34 SMM 3, we took an additional spectrum at its position [ $\alpha(J2000) = 05^h47^m05^s.2$ ,  $\delta(J2000) = +21^\circ00'25''$ ] on 2004 August 25, to try to determine with which source the maser emission was more likely to be related to. However, the spectrum was similar (peak intensity  $\simeq 0.32 \pm 0.13 \text{ mJy}$  at  $7.7 \text{ km s}^{-1}$ ) to the one obtained at CB 34 SMM 3 the same day (Table 2). Therefore, it is not possible to ascertain the association of the maser with either submillimeter source, and since the signal-to-noise ratio of the spectra was relatively low, any other attempt to determine a more precise position would have been subject to high uncertainties. The water maser may in fact be pumped by a source lying roughly at the same distance from SMM 3 and SMM 4. A good candidate could be source Q, also lying within the telescope beam from both submillimeter sources (at  $\sim 13''$  from them), and which Moreira & Yun (1995) suggested to be the powering source of one of the jet-like chains of  $\text{H}_2$  knots (Q knots). Interestingly, this jet is the one whose orientation is closer to that of the molecular outflow. Therefore, this Q-jet could trace the dominant mass-loss process in CB 34. No interferometric observations of the maser emission have been carried out so far. These observations would be useful to determine the excitation source of the maser and to relate the water maser distribution with that of the jets in the region.

#### 4.2.3. CB 54 ([YMT96] CB 54 2)

CB 54 (LBN 1042), located at 1.5 kpc (Launhardt & Henning 1997), is an active site of star formation, with multiple jets (Khanzadyan 2003) and a bipolar outflow (Yun & Clemens 1992, 1994a). We detected water maser emission towards the centimeter source [YMT96] CB 54 2 (also named as [YMT96] CB 54 VLA 1; Yun et al. 1996; Moreira et al. 1997). Within the beam of the Robledo telescope also fall IRAS 07020-1618, a mm source (Launhardt & Henning 1997), a submillimeter source (Launhardt et al. 1997), the peak of a CS map (Launhardt et al. 1998), and the geometrical center of the molecular outflow (Yun & Clemens 1992, 1994a). This radio continuum source is associated with the near-infrared source CB54YC1 (Yun & Clemens 1994b, 1995). This source is in its turn composed of at least two individual near-infrared objects, surrounded by a common nebulosity, and has been proposed to be an embedded binary system of class I YSOs (Yun 1996).

The maser emission is highly variable. On 2002 May and 2003 May, the flux density was below 1 Jy. However, a component at  $\simeq 7.9 \text{ km s}^{-1}$ , undetected on 2002 May, suffered an outburst in 2003 June-July, reaching a flux density of  $\simeq 50 \text{ Jy}$ . This component was again undetected (or very weak and blended with a component at  $8.7 \text{ km s}^{-1}$ ) on 2005 April. Such high variability in a water maser is typical of a low-mass YSO (see e.g., Wilking et al 1994). The velocity of the maser emission is within  $15 \text{ km s}^{-1}$  from the cloud velocity ( $V_{\text{LSR}} \simeq 19.5 \text{ km s}^{-1}$ , CB).

#### 4.2.4. CB 65 (IRAS 16277-2332)

CB 65 (LDN 1704) is at a distance of  $\sim 160 \text{ pc}$  (Visser et al. 2002), which makes it the nearest cloud among our detections. We detected maser emission towards IRAS 16277-2332. There is no other source complying our selection criteria within the Robledo beam around this IRAS source. Moreover, there is not much known about IRAS 16277-2332, apart from its non-detection in the submillimeter (Visser et al. 2002), and that Parker (1989) does not include it as associated with CB 65, so we cannot say much about the nature of this source. Moreover, DG06 did not find high-velocity wings in the CO spectra towards IRAS 16277-2332 that could indicate the presence of an outflow from a YSO. This IRAS source was classified in CB as envelope type (i.e., not within the visible boundaries of the globule) and is detected only at  $60 \mu\text{m}$ , with only 0.92 Jy, which is at the detection limit.

The maser was detected in 2002 June, but it was not visible in later observations with the Robledo radio telescope (Table 2), or with the VLA (on 2005 February 12, DG06). The lack of evidence for outflow activity, and the possible non-association of IRAS 16277-2332

with the globule, suggest that this source could be an evolved object, although there are not enough infrared and optical data to support this suspicion (DG06). However, it is worth noting that the maser velocity ( $V_{\text{LSR}} \simeq 1.2 \text{ km s}^{-1}$ , Table 2) is close to the velocity of the cloud ( $V_{\text{LSR}} \simeq 2.3 \text{ km s}^{-1}$ , CB), which would be very unlikely if the object is completely unrelated to the globule.

#### 4.2.5. CB 101 (IRAS 17503-0833)

CB 101 (LDN 392) is a globule located at 200 pc (Lee & Myers 1999). Lee & Myers (1999) and Lee, Myers, & Tafalla (2000) cataloged it as a starless core.

We detected maser emission towards IRAS 17503-0833. No other source with our selection criteria is found around this IRAS source. The maser does not show strong variations in flux density, although it showed a double-peaked profile in 2002, of which only one component was visible in 2004. The maser emission, at  $V_{\text{LSR}} \simeq 29 \text{ km s}^{-1}$  (Table 2), is  $\gtrsim 20 \text{ km s}^{-1}$  away from the cloud velocity ( $\simeq 6.7 \text{ km s}^{-1}$ , CB). We note that the centroid velocities of water maser emission from YSOs, specially for low-mass sources, is usually found within  $\simeq 15 \text{ km s}^{-1}$  from the cloud velocity (Wilking et al 1994; Anglada et al. 1996; Brand et al. 2003). The high relative velocity of the maser emission in this source with respect to the LSR velocity of the CB 101 globule, suggests that its pumping source may not be associated with the globule. By inspecting the optical images of the Digital Sky Survey, we noted that IRAS 17503-0833 is out of the optical limit of CB 101, and it should probably not have been included in the list of IRAS sources of CB.

Due to the lack of high-velocity CO emission and of local enhancement of molecular gas towards IRAS 17503-0833, and based on its spectral energy distribution, DG06 suggested that this source could be a Mira variable star, rather than a YSO.

#### 4.2.6. CB 199 ([ARC2001] HH 119 VLA 3)

CB 199 (B335), located at 250 pc (Tomita, Saito, & Ohtani 1979) is an extensively studied site of recent star formation, which has also been the subject of spectral line studies of protostellar collapse (Zhou et al. 1993; Choi et al. 1995).

There is a bipolar molecular outflow in the region (Frerking & Langer 1982; Goldsmith et al. 1984), as well as the jet-like structure of Herbig-Haro objects HH 199A, B, and C (Vrba et al. 1986; Reipurth et al. 1992). Both the molecular outflow and the optical jet are thought to be powered by a far-infrared and submillimeter source (Keene et al. 1983;

Chandler et al. 1990), which is probably the same object as IRAS 19345+0727. A total of 13 centimeter sources were detected around this IRAS source (Anglada et al. 1992, 1998; Avila, Rodríguez, & Curiel 2001) of which at least 4 are probably background objects due to their non-thermal, negative spectral index at radio wavelengths (Anglada et al. 1998).

We detected maser emission towards ([ARC2001] HH 119 VLA 3), a radio continuum source of  $\simeq 0.55$  mJy detected by Avila, Rodríguez, & Curiel (2001), but undetected in the previous observations by Anglada et al. (1992) and Anglada et al. (1998) (upper limit of  $\sim 0.15$  mJy), which suggested source variability. No other source with our selection criteria was known within the beam of Robledo from this source. The other radio continuum sources in the region are more than  $2'$  away from this one. The radio continuum source [ARC92] Barn 335 4 (Anglada et al. 1992), associated with IRAS 19345+0727, the powering source of the outflow, lies  $\simeq 3'.5$  from [ARC2001] HH 119 VLA 3. Therefore, the water maser seems not to be related with either this outflow or the HH 199 jet. The lack of infrared counterpart for [ARC2001] HH 119 VLA 3 in the IRAS point source and 2MASS catalogs would suggest that this object is deeply embedded, and thus, very young.

Only one maser component at  $\simeq 37.9$  km s $^{-1}$  is clearly visible in our spectra. This is  $\sim 30$  km s $^{-1}$  from the cloud velocity (8.4 km s $^{-1}$ , CB), i.e., a shift for the centroid velocity much larger than expected for masers in YSOs (Wilking et al 1994; Anglada et al. 1996; Brand et al. 2003). Although they are rare, there are some known cases of sources with large velocity shifts (up to  $\simeq 80$  km s $^{-1}$ ) between water masers and cloud, specially around HH and GGD objects Rodríguez et al. (1978, 1980), but they are generally associated with high-mass YSOs. Large velocity shifts are even rarer in low-mass objects. If the maser is associated with a YSO in the globule CB 199, this would be one of the cases with the largest velocity offset between maser emission and cloud velocity known to date for a low-mass star-forming region. A similar, unusual shift of  $\simeq 30$  km s $^{-1}$  is also found in the low-mass YSO SVS13 (Claussen et al. 1996), while values  $\simeq 45$  km s $^{-1}$  have been seen in Cep E-mm (Furuya et al. 2003), although the latter is probably an intermediate-mass YSO ( $\sim 3 M_{\odot}$ ; Moro-Martín et al 2001; Froebrich et al. 2003). Both SVS13 and Cep E-mm seem to be close binaries, with separations of  $\simeq 65$  AU (Anglada, Rodríguez, & Torrelles 2000; Eisloffel et al 1996). In the case SVS13, Rodríguez et al. (2002) showed that the high-velocity masers seem to be associated with one of the components, although the maser velocities do not seem to mark the orbital motions in the binary, given the low-mass of the system. On the other hand, it has been proposed that gravitational interactions within binaries or multiple systems give rise to mass-loss outbursts that show up as Herbig Haro jets or FU Ori phenomena (Reipurth 2000; Reipurth & Aspin 2004), and we could speculate that these outbursts could also show up as high-velocity masers. However, it is not possible at this point to determine whether high-velocity masers are favored in low-mass binary systems, given the scarce number of

objects we are dealing with. Obviously, it would be interesting to determine whether the source [ARC2001] HH 119 VLA 3 is indeed a binary.

An alternative possibility to explain this high-velocity feature is that [ARC2001] HH 119 VLA 3 is associated with an evolved star. If this is true, and the source [ARC2001] HH 119 VLA 3 is the one pumping the maser, the presence of radio continuum emission would indicate that it is a protoplanetary or a young planetary nebula, located behind the CB 199 globule. It is not likely that it is an evolved object in the foreground (i.e., closer than 250 pc), given the lack of an infrared counterpart.

There are no further interferometric observations of the maser in this source by DG65. Given the proximity of CB 199, and the abnormal velocity pattern, such interferometric observations would be useful to confirm its association with the radio continuum source and the spatio-kinematical distribution of the maser emission.

#### 4.2.7. CB 232 (*IRAS 21352+4307*)

CB 232 is a globule located at 600 pc (Launhardt & Henning 1997). We detected a maser towards IRAS 21352+4307. From the nominal position of this source, within the beam of Robledo fall two submm sources ([HSW99] CB 232 SMM 1 and SMM 2, Huard et al. 1999), the peak of a CS map (Launhardt et al. 1998), and the center of a molecular outflow (Yun & Clemens 1992, 1994a).

The maser emission shows a varying velocity pattern. The maximum emission was at  $\simeq 12.1$  km s<sup>-1</sup> in 2003 May, although a weaker component at  $\simeq 10$  km s<sup>-1</sup> was also present. This weaker component was the dominant one in later spectra, while the one at 12.1 km s<sup>-1</sup> was absent. The detected maser components are close to the cloud velocity ( $\simeq 12.6$  km s<sup>-1</sup>, CB).

The variation of the maser spectrum and the presence of other signs of star formation indicates that the maser emission is pumped by a low-mass YSO. There is a near-infrared infrared source (CB232YC1-I), classified as a class I object by Yun & Clemens (1995), and located between SMM 1 and SMM 2, and at  $\simeq 10''$  and  $\simeq 5''$  from each of them, respectively. The identification of CB232YC1-I with SMM 2 is uncertain, given the positional uncertainty of the latter ( $\simeq 4''$  Huard et al. 1999). Therefore, there are at least 2 objects within  $10''$ . Further interferometric observations of the water maser (DG06) found this emission to lie at the position of CB232YC1-I, which confirms that this class I source could be the powering source of the molecular outflow.

## 5. Discussion

Of the selection criteria used to select our target sources, the highest detection rates of masers are those related to the presence of molecular outflows or the peak in maps of the high-density tracer CS. We performed a statistical study to try to determine whether any of the selection criteria is a better predictor for the presence of water maser emission. For this, we used a Fisher’s Exact test and a 95% confidence level. This test indicates that the presence of a submillimeter source, of a peak of CS, or of a molecular outflow are all a better predictor of the existence of water maser emission than the presence of an IRAS source, which is reasonable, since the latter was the less restrictive of all our criteria in the identification of YSOs candidates. Apart for IRAS sources, the detection rates for all other selection criteria (even the 0% rate for peaks of  $\text{NH}_3$  maps) are all statistically compatible.

Another relevant fact is that most of the globules in the CB catalog which are known to be associated with water masers (CB 3, CB 34, CB 39, CB 54, CB 205) are located at distances  $\geq 1$  kpc. Therefore, they tend to be larger than probably intended by CB in their catalog, which tried to select “small” (size  $\lesssim 1.5$  pc) globules, using a criterion of  $< 10'$  assuming distances  $\lesssim 500$  pc. So the globules mentioned above belong to a class of “large” Bok globules. Large, massive globules are obviously more likely to be sites of star formation, with a larger number of YSOs, and therefore, with a higher probability of hosting at least one water-maser-emitting object. YSOs in larger globules would also tend to be more massive (as in the case of CB 3) than in the case of smaller globules, which also increases the probability of the presence of water masers. In our survey we have identified the smallest Bok globules known to harbor water maser emission. In particular, CB 232, whose maser is most likely associated with a YSO, has a size of  $\simeq 0.6$  pc ( $5'.6 \times 2'.2$  at 600 pc; CB; Launhardt & Henning 1997). The cases of CB 65 ( $\simeq 0.3$  pc size) and CB 199 ( $\simeq 0.5$  pc size) need further investigation to determine the nature of their pumping sources, but these three sources seem to be the best candidates for further use of water masers as a tool to study star formation in small Bok globules.

## 6. Conclusions

In this paper, we present the most sensitive survey for water maser emission towards Bok globules to date, using NASA’s 70m antenna in Robledo de Chavela (Spain). A total of 203 target positions within the clouds of the Clemens & Barvainis (1988) catalogs were observed. Our main results are as follow:

- We have obtained 7 maser detections, 6 of which (in CB 34, CB 54, CB 65, CB 101,

CB 199, and CB 232) are new. Of the previously known masers in the CB catalog, only the one in CB 3 was detected by us. No emission was seen towards the previously reported masers in either CB 39 or CB 205.

- Of our detections, the ones in CB 3, CB 34, CB 54, and CB 232 are most likely associated with YSOs. We suggest that the maser in CB 101 is associated with an evolved object. The nature of CB 65 is uncertain.
- In the case of CB 199, the relatively large shift ( $\simeq 30 \text{ km s}^{-1}$ ) of the centroid velocity of the maser emission with respect to the cloud velocity is unusual for YSOs, specially for low-mass ones. We speculate that the presence of high-velocity masers in low-mass YSOs might be related with episodes of energetic mass loss in close binaries. Alternatively, the maser in CB 199 could be related to a protoplanetary or a young planetary nebula.
- CB 232 is the smallest Bok globule (size  $\simeq 0.6 \text{ pc}$ ) known to be associated with water maser emission. However, if their association with YSOs is confirmed, CB 65 (size  $\simeq 0.3 \text{ pc}$ ) and CB 199 ( $\simeq 0.5 \text{ pc}$ ) are even smaller globules. These objects are good candidates for the study of relatively isolated star formation with high spatial resolution.
- Of our selection criteria, the more restrictive ones for the identification of YSOs (radio continuum emission, peak of a high-density tracer, and geometrical center of a molecular outflow) show statistically compatible rates of water maser detection. Only the presence of IRAS sources tends to be a somewhat worse predictor for the presence of masers.

We are deeply indebted to many staff members at the Madrid Deep Space Communication Complex and Jet Propulsion Laboratory, without whose invaluable help spectroscopy observations at Robledo (and therefore this paper) would have never been possible. We would also like to thank the water megamaser group at the Harvard-Smithsonian Center for Astrophysics (Lincoln Greenhill, Paul Kondratko, and James Moran) for allowing us to use their SAO-4K spectrometer during four nights in which our 256-channel spectrometer was not working. We also thank Paul Kondratko for providing us with his SAO-4K data processing software, which was useful to develop ours for the 384-channel spectrometer (SPB500). JFG acknowledges support from MEC (Spain) grant AYA 2005-08523-C03-03 and from Junta de Andalucía (TIC-126). OS is partially supported by MEC grant AYA2003-09499. IdG acknowledges the support of a Calvo Rodés predoctoral fellowship from the Instituto Nacional de Técnica Aeroespacial during the development of this work. This paper is based on observations taken during “host-country” allocated time at Robledo de Chavela;

this time is managed by the LAEFF of INTA, under agreement with NASA/INSA. It also makes use of data products from the Two Micron All Sky Survey (2MASS), which is a joint project of the University of Massachusetts and the Infrared Processing and Analysis Center at the California Institute of Technology, funded by NASA and the NSF. We acknowledge the use of the free GILDAS software of IRAM (<http://www.iram.fr/IRAMFR/GILDAS>) for data reduction of our spectral line data. This research has also made use of the SIMBAD database, operated at CDS, Strasbourg, France.

## REFERENCES

- Alves, J. F., & Yun, J. L. 1995, *ApJ*, 438, L107
- André, P., Ward-Thompson, D., & Barsony, M. 1993, *ApJ*, 406, 122
- Anglada, G., Estalella, R., Pastor, J., Rodríguez, L. F., & Haschick, A. D. 1996, *ApJ*, 463, 205
- Anglada, G., Rodríguez, L. F., Cantó, J., Estalella, R., & Torrelles, J. M. 1992, *ApJ*, 395, 494
- Anglada, G., Rodríguez, L. F., & Torrelles, J. M. 2000, *ApJ*, 542, L123
- Anglada, G., Rodríguez, L. F., Torrelles, J. M., Estalella, R., Ho, P. T. P., Cantó, J., López, R., & Verdes-Montenegro, L. 1989, *ApJ*, 341, 208
- Anglada, G., Villuendas, E., Estalella, R., Beltrán, M. T., Rodríguez, L. F., Torrelles, J. M., & Curiel, S. 1998, *AJ*, 116, 2953
- Armstrong, J. T., & Winnewisser, G. 1989, *A&A*, 210, 373
- Avila, R., Rodríguez, L. F., & Curiel, S. 2001, *Rev. Mex. AA*, 37, 201
- Benson, P. J., & Myers, P. C. 1989, *ApJS*, 71, 89
- Benson, P. J., Myers, P. C., & Wright, E. L. 1984, *ApJ*, 279, L27
- Bok, B. J., & Reilly, E. F. 1947, *ApJ*, 105, 255
- Bontemps, S., André, P., Terebey, S., & Cabrit, S. 1996, *A&A*, 311, 858
- Bourke, T. L., Hyland, A. R., & Robinson, G. 1995, *MNRAS*, 276, 1052 (BHR)

- Bourke, T. L., Hyland, A. R., Robinson, G., James, S. D., & Wright, C. M. 1995, *MNRAS*, 276, 1067
- Brand, J., Cesaroni, R., Comoretto, G., Felli, M., Palagi, F., Palla, F., & Valdetaro, R. 2003, *A&A*, 407, 573
- Chandler, C. J., Gear, W. K., Sandell, G., Hayashi, S., Duncan, W. D., Griffin, M. J., & Hazell, A. S. 1990, *MNRAS*, 243, 330
- Choi, M., Evans, N. J., II, Gregerson, E. M., & Wang, Y. 1995, *ApJ*, 448, 742
- Clarke, C., Reipurth, B., & Delgado-Donate, E. 2004, *Rev. Mex. AA. SC*, 21, 184
- Claussen, M. J., Wilking, B. A., Benson, P. J., Wootten, A., Myers, P. C., & Terebey, S. 1996, *ApJS*, 106, 111
- Claussen, M. C., Wootten, H. C., Brogan, C. L., Marvel, K. B., & Furuya, R. S. 2005, in *ASP Conf. Ser. 340: Future Directions in High Resolution Astronomy*, eds. J. Romney & M. Reid (ASP: San Francisco), 324
- Clemens, D. P., & Barvainis, R. 1988, *ApJS*, 68, 257 (CB)
- Clemens, D. P., Yun, J. L., & Heyer, M. H. 1991, *ApJS*, 75, 877
- Codella, C., & Bachiller, R. 1999, *A&A*, 350, 659
- Codella, C., Palumbo, G. G. C., Pareschi, G., Scappini, F., Caselli, P., & Attolini, M. R. 1995, *MNRAS*, 276, 57
- Codella, C., & Scappini, F. 1998, *MNRAS*, 298, 1092
- de Gregorio-Monsalvo, I., Gómez, J. F., Suárez, O., Kuiper, T. B. H., Anglada, G., Patel, N.A., & Torrelles, J. M. 2006, *AJ Submitted* (DG06)
- Eisloffel, J., Smith, M. D., Davis, C. J., & Ray, T. P. 1996, *AJ*, 112, 2086
- Felli, M., Palagi, F., & Tofani, G. 1992, *A&A*, 255, 293
- Froebrich, D., Smith, M. D., Hodapp, K.-W., & Eisloffel, J. 2003, *MNRAS*, 346, 163
- Frerking, M. A. & Langer, W. D. 1982, *ApJ*, 256, 523
- Furuya, R. S., Kitamura, Y., Wootten, H. A., Claussen, M. J., & Kawabe, R. 2001, *ApJ*, 559, L143

- Furuya, R. S., Kitamura, Y., Wootten, A., Claussen, M. J., & Kawabe, R. 2003, *ApJS*, 144, 71
- Goldsmith, P. F., Snell, R. L., Hemeon-Heyer, M., & Langer, W. D. 1984, 286, 599
- Gómez, J. F., Curiel, S., Torrelles, J. M., Rodríguez, L. F., Anglada, G., & Girart, J. M. 1994, *ApJ*, 436, 749
- Harvey, D. W. A., Wilner, D. J., Di Francesco, J., Lee, C. W., Myers, P. C., & Williams, J. P. 2002, *AJ*, 123, 3325
- Huard, T. L., Sandell, G., & Weintraub, D. A., 1999, *ApJ*, 526, 833
- Huard, T. L., Weintraub, D. A., & Sandell, G. 2000, *A&A*, 362, 635
- Jijina, J., Myers, P. C., & Adams, F. C. 1999, *ApJS*, 125, 161
- Keene, J., Davidson, J. A., Harper, D. A., Hildebrand, R. H., Jaffe, D. T., Loewenstein, R. F., Low, F. J., & Pernic, R. 1983, *ApJ*, 274, L43
- Khanzadyan, T. 2003, in *Communications of the Konkoly Observatory 103, The interaction of stars with their environment II*, eds. C. Kiss, M. Kun, & V. Könyves (Konkoly Observatory: Budapest), 31
- Khanzadyan, T., Smith, M. D., Gredel, R., Stanke, T., & Davis, C. J. 2002, *A&A*, 383, 502
- Launhardt, R. Evans, N. J., II., Wang, Y., Clemens, D. P., Henning, Th., & Yun, J. L. 1998, *ApJS*, 119, 59
- Launhardt, R., & Henning, T. 1997, *A&A*, 326, 329
- Launhardt, R., Ward-Thompson, D., & Henning, Th. 1997, *MNRAS*, 288, L45
- Lee, C. W., & Myers, P. C. 1999, *ApJS*, 123, 233
- Lee, C. W., Myers, P. C., & Tafalla, M. 1999, *ApJ*, 526, 788
- Lemme, C., Wilson, T. L., Tiefertunk, A. R., & Henkel, C. 1996, *A&A*, 312, 585
- Martin, R. N. & Barrett, A. H. 1978, *ApJS*, 36, 1
- Massi, F., Codella, C., & Brand, J. 2004, *A&A*, 419, 241
- Moreira, M. C., & Yun, J. L. 1995, *ApJ*, 454, 850

- Moreira, M. C., Yun, J. L., Torrelles, J. M., Afonso, J. M., & Santos, C. A. 1999, *AJ*, 118, 1315
- Moreira, M. C., Yun, J. L., Vázquez, R. Torrelles, J. M., 1997, *AJ*, 113, 1371
- Moro-Martín, A., Noriega-Crespo, A., Molinari, S., Testi, L., Cernicharo, J., & Sargent, A. 2001, *ApJ*, 555, 146
- Neckel, T., Chini, R., Güsten, R., & Wink, J. E. 1985, *A&A*, 153, 253
- Palla, F., & Prusti, T. 1993, *A&A*, 272, 249
- Parker, N. D. 1989, *MNRAS*, 235, 139
- Persi, P., Palagi, F., & Felli, M. 1994, *A&A*, 291, 577P
- Reipurth, B. 2000, *AJ*, 120, 3177
- Reipurth, B., & Aspin, C. 2004, *ApJ*, 608, L65
- Reipurth, B., Heathcote, S., & Vrba, F. 1992, *ApJ*, 256, 225
- Scappini, F., Caselli, P., & Palumbo, G. G. C. 1991, *MNRAS*, 249, 763
- Schwartz, P. R. & Buhl, D. 1975, *ApJ*, 201, L27
- Rodríguez, L. F., Anglada, G., Torrelles, J. M., Mendoza-Torres, J. E., Haschick, A. D., & Ho, P. T. P. 2002, *A&A*, 389, 572
- Rodríguez, L. F., Moran, J. M., Dickinson, D. F., & Gyulbudaghian, A. L. 1978, *ApJ*, 226, 115
- Rodríguez, L. F., Moran, J. M., Gottlieb, E. W., Ho, P. T. P. 1980, *ApJ*, 235, 845
- Saraceno, P., André, P., Ceccarelli, C., Griffin, M., & Molinari, S. 1996, *A&A*, 309, 827
- Terebey, S., Vogel, S. N., & Myers, P. C. 1992, *ApJ*, 390, 181
- Tomita, Y., Saito, T., & Ohtani, H. 1979, *PASJ*, 31, 407
- Torrelles, J. M., Gómez, J. F., Garay, G., Rodríguez, L. F., Curiel, S., Cohen, R. J., & Ho, P. T. P. 1998, *ApJ*, 509, 262
- Torrelles, J. M., Gómez, J. F., Rodríguez, L. F., Ho, P. T. P., Curiel, S., & Vázquez, R. 1997, *ApJ*, 489, 744

- Torrelles, J. M., Patel, N. A., Gómez, J. F., & Anglada, G. 1992, *Rev. Mex. AA Ser. Conf.*, 13, 108
- Vallée, J. P., Bastien, P., & Greaves, J. S. 2000, *ApJ*, 542, 352
- Visser, A. E., Richer, J. S., & Chandler, C. J. 2001, *MNRAS*, 323, 257
- Visser, A. E., Richer, J. S., & Chandler, C. J. 2002, *AJ*, 124, 2756
- Vrba, F. J., Luginbuhl, C. B., Strom, S. E., Strom, K. M., & Heyer, M. H. 1986, *AJ*, 92, 633
- Wiling, B. A. & Claussen, M. J. 1987, *ApJ*, 320, L133
- Wiling, B. A., Claussen, M. J., Benson, P. J., Myers, P. C., Terebey, S., & Wootten, A. 1994, *ApJ*, 431, L119
- Wiling, B. A., Lada, C. J., & Young, E. T. 1989, *ApJ*, 340, 823
- Wouterloot, J. G. A., Brand, J., & Fiegle, K. 1993, *A&AS*, 98, 589
- Yun, J. L. 1996, *AJ*, 111, 930
- Yun, J. L. & Clemens, D. P. 1991, *ApJ*, 365, L73
- Yun, J. L., & Clemens, D. P. 1992, *ApJ*, 385, L21
- Yun, J. L., & Clemens, D. P. 1994a, *ApJS*, 92, 145
- Yun, J. L., & Clemens, D. P. 1994b, *AJ*, 108, 612
- Yun, J. L., & Clemens, D. P. 1995, *AJ*, 109, 742
- Yun, J. L., Moreira, M. C., Torrelles, J. M., Afonso, J. M., & Santos, N. C. 1996, *AJ*, 111, 841
- Zhou, S., Evans, N. J., II, Kömpe, C., & Walmsley, C. M. 1993, *ApJ*, 404, 232

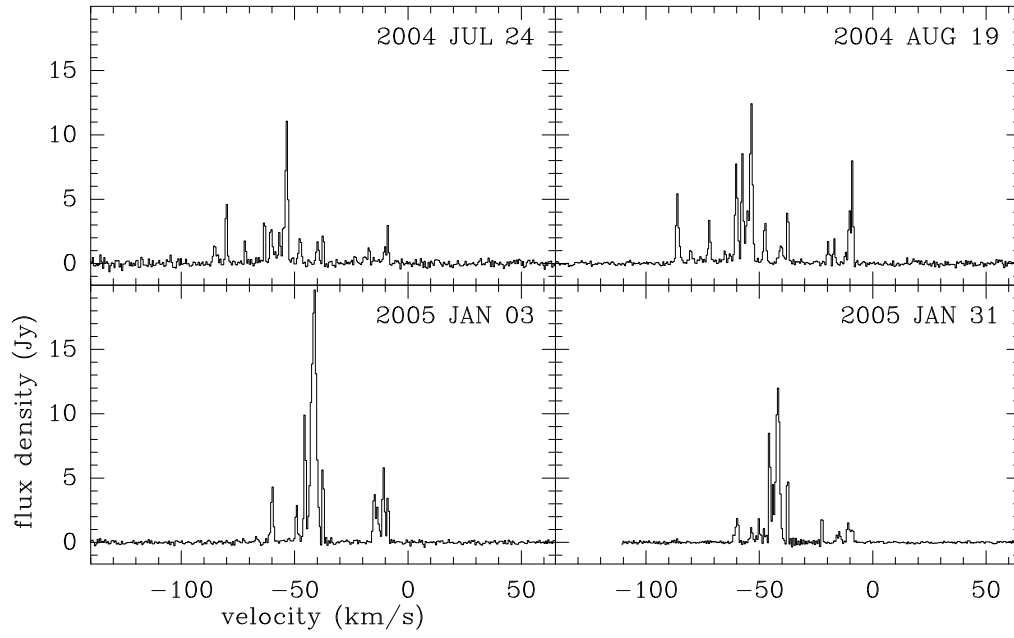


Fig. 1.— Water maser spectra towards CB3-mm

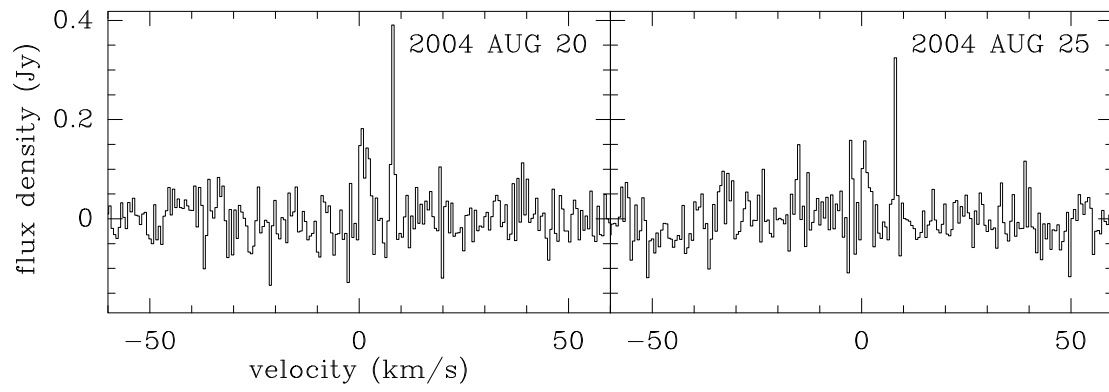


Fig. 2.— Water maser spectra towards [HSW99] CB 34 SMM 3

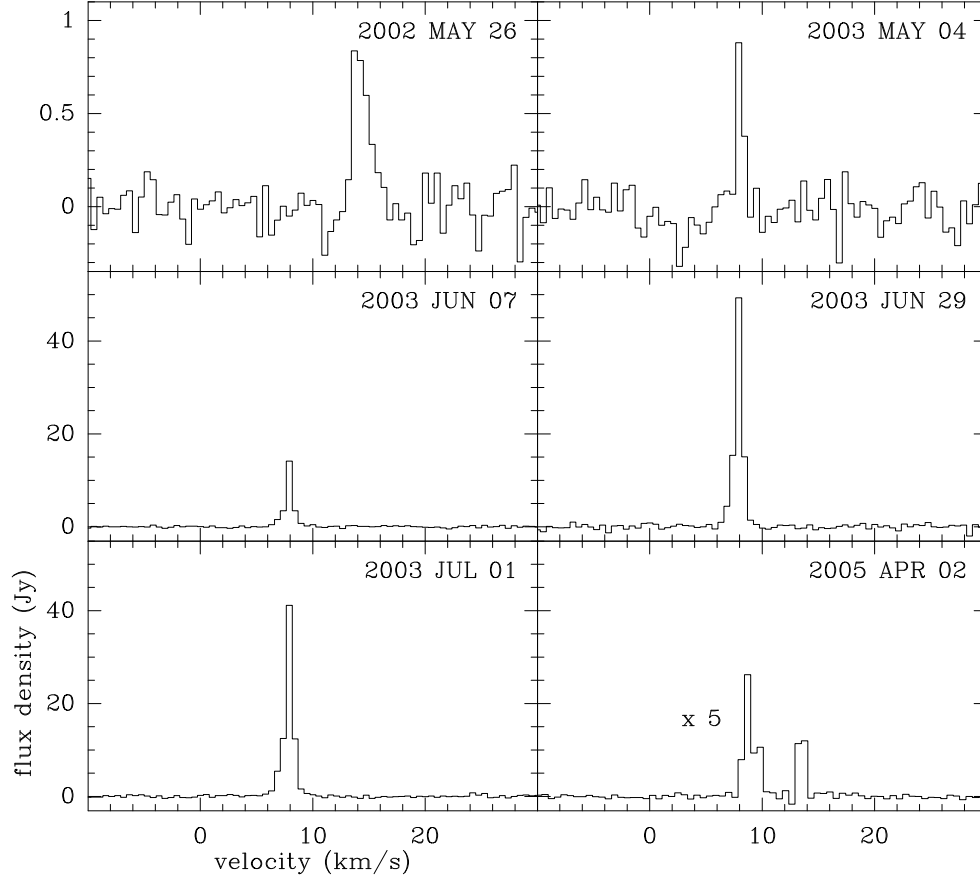


Fig. 3.— Water maser spectra towards [YMT96] CB 54 2. Note that the scale of the top panels is different from the rest. The spectrum taken on 2005 April 02 (bottom right) has been multiplied by a factor of 5 to show it more clearly

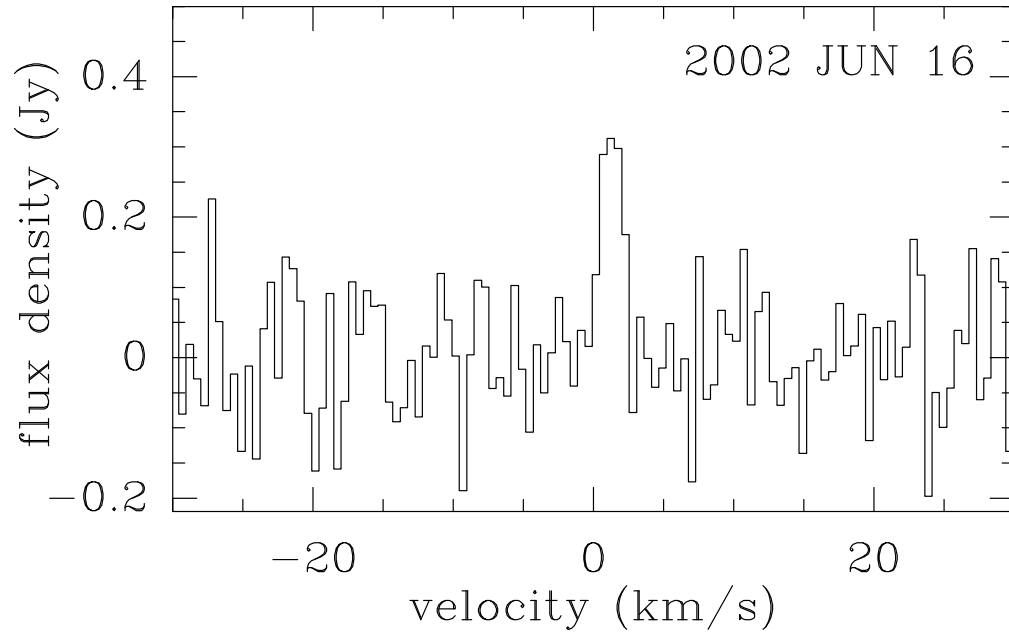


Fig. 4.— Water maser spectrum towards IRAS 16277-2332 in CB 65

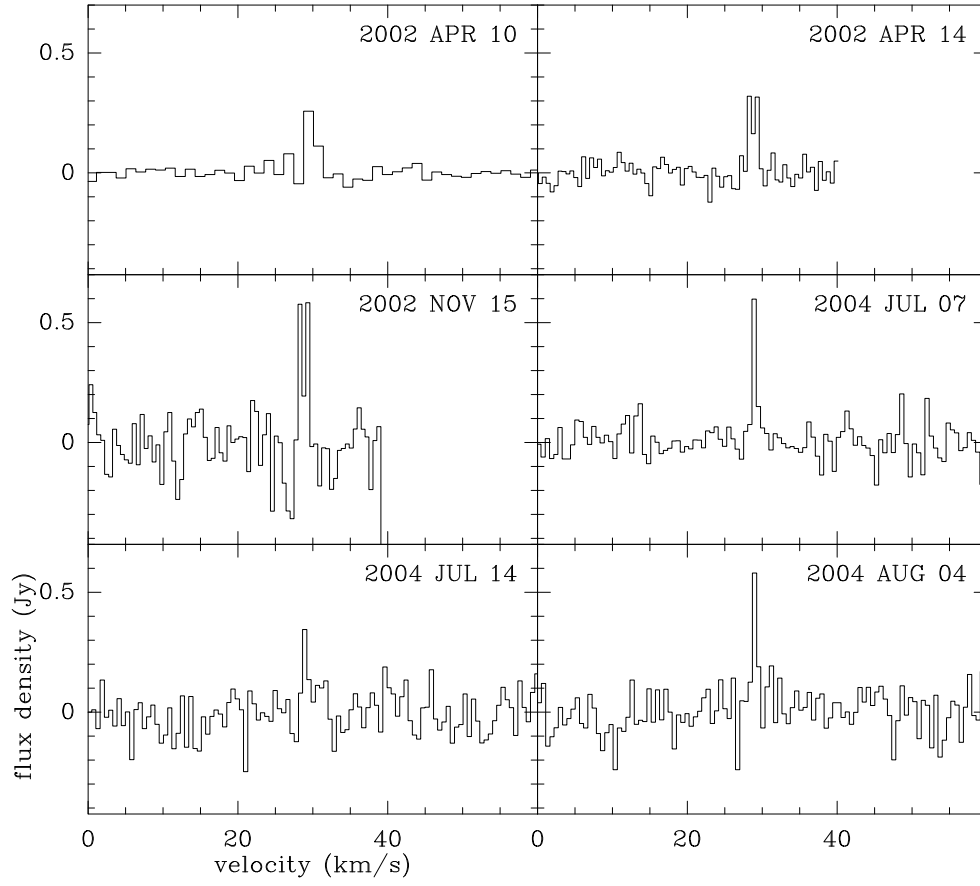


Fig. 5.— Water maser spectra towards IRAS 17503-0833 in CB 101

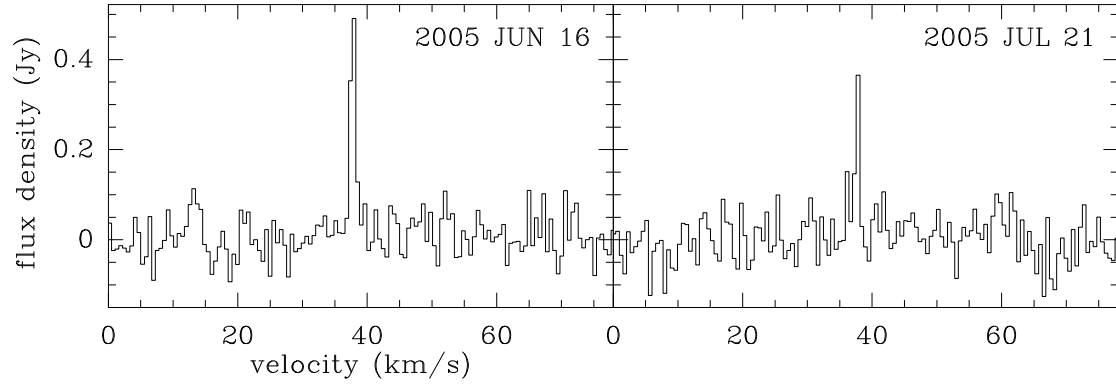


Fig. 6.— Water maser spectra towards [ARC2001] HH 119 VLA 3 in CB 199

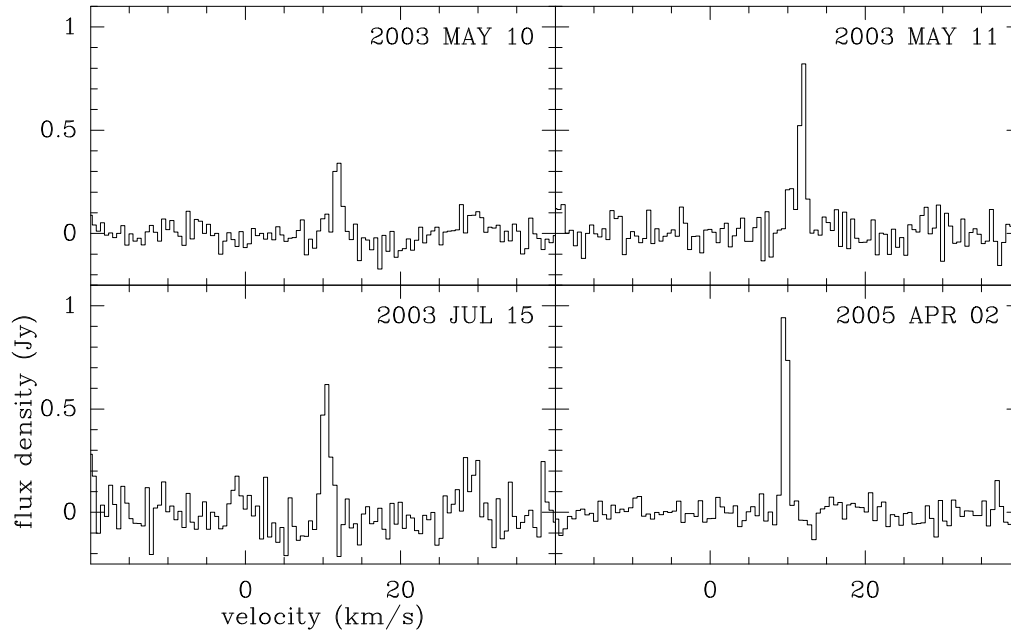


Fig. 7.— Water maser spectra towards IRAS 21352+4307 in CB 232

Table 1. Sources searched for water maser emission

Globule	Source <sup>a</sup>	Right Ascension <sup>b</sup> (J2000)	Declination <sup>b</sup> (J2000)	Included Sources <sup>c</sup>	References <sup>d</sup>
CB 3	[YMT96] CB 3 1	00 28 22.0	+56 41 39		6
	CB3-mm <sup>e</sup>	00 28 42.7	+56 42 06	smm ([HSW99] CB 3 SMM 1), IRAS 00259+5625, outf, cs	1, 2, 3, 4, 5
CB 4	IRAS 00362+5234	00 39 03.5	+52 50 57		
CB 6	IRAS 00465+6028	00 49 25.0	+50 44 45	mm, smm	1, 2
CB 7	IRAS 01078+6409	01 11 03.4	+64 25 24		
	IRAS 01087+6404	01 11 58.0	+64 20 07		
CB 8	IRAS 01202+7406	01 24 12.4	+74 22 03		
CB 11	IRAS 01333+6448	01 36 51.5	+65 03 55		
	IRAS 01334+6442	01 36 59.4	+64 57 39		
	IRAS 01341+6447	01 37 41.3	+65 03 08		
CB 12	CS peak	01 38 32.7	+65 06 02		5
	IRAS 01354+6447	01 38 56.8	+65 03 12		
CB 15	IRAS 03521+5555	03 56 07.9	+56 04 30		
	IRAS 03523+5608	03 56 21.7	+56 17 01		
	IRAS 03535+5555	03 57 30.4	+56 04 15		
CB 16	IRAS 03592-5642	04 03 15.6	+56 50 27		
CB 17	IRAS 04005+5647	04 04 33.7	+56 56 10	mm, smm	1, 2
	NH <sub>3</sub> peak	04 04 38.0	+56 56 11		7
CB 19	IRAS 04233+2529	04 26 21.3	+25 36 22		
	IRAS 04240+2535	04 27 02.7	+25 42 24		
CB 22	NH <sub>3</sub> peak	04 40 33.2	+29 55 04		7
CB 23	NH <sub>3</sub> peak	04 43 30.0	+29 39 01		7
	CB23-cm1	04 43 34.9	+29 38 05		8
	CB23-cm2	04 43 35.0	+29 37 13		8
CB 26	IRAS 04559+5200	04 59 52.4	+52 04 45	mm	1
CB 27	IRAS 05013+3234	05 04 37.2	+32 38 15		
CB 28	IRAS 05036-0359	05 06 08.9	−03 55 16		
	IRAS 05037-0402	05 06 13.7	−03 58 60		
	CS peak	05 06 19.4	−03 56 24	IRAS 05038-0400	
	IRAS 05038-0400	05 06 19.9	−03 56 33	cs	5
	NH <sub>3</sub> peak	05 06 20.2	−03 56 02		7
CB 29	IRAS 05190-0348	05 21 31.5	−03 45 08		
	IRAS 05194-0346	05 21 56.2	−03 44 08		5
	IRAS 05194-0343	05 21 57.5	−03 40 35		

Table 1—Continued

Globule	Source <sup>a</sup>	Right Ascension <sup>b</sup> (J2000)	Declination <sup>b</sup> (J2000)	Included Sources <sup>c</sup>	References <sup>d</sup>
	CS peak	05 22 10.3	−03 41 06		5
	IRAS 05201-0341	05 22 38.5	−03 38 53		
CB 30	[MYT99] CB 30 3	05 29 30.5	+05 43 22		9
	IRAS 05268+0550	05 29 31.7	+05 52 55		
	IRAS 05268+0538	05 29 32.2	+05 40 34	cm ([MYT99] CB30 4), cs	9, 5
	IRAS 05274+0542	05 30 06.7	+05 44 23		
CB 31	[YMT96] CB 31 1	05 33 14.5	−00 35 34		6
	[YMT96] CB 31 2	05 33 15.8	−00 35 20		6
	IRAS 05307-0038	05 33 18.2	−00 36 13		
CB 32	IRAS 05344-0016	05 36 59.7	−00 14 21		
	CS peak	05 38 28.2	−00 17 25		5
CB 33	IRAS 05433+2040	05 46 17.7	+20 41 39		
	IRAS 05437+2045	05 46 41.1	+20 46 10		
CB 34	[HSW99] CB 34 SMM 2	05 47 00.0	+21 00 30		3
	[YMT96] CB 34 3	05 47 01.7	+21 00 25	mm, smm ([HSW99] CB 34 SMM 1), IRAS 05440+2059, outf, cs, nh3	6, 1, 2, 3, 4, 5, 10
	[HSW99] CB 34 SMM 1	05 47 01.9	+21 00 06	cm ([YMT96] CB 34 3), IRAS 05440+2059	3, 6
	[HSW99] CB 34 SMM 3	05 47 05.3	+21 00 42	smm ([HSW99] CB 34 SMM 4)	3
	[HSW99] CB 34 SMM 5	05 47 07.8	+21 00 04		3
CB 37	[MYT99] CB 37 1	06 00 35.6	+31 37 37		11
	NH <sub>3</sub> peak	06 00 37.3	+31 38 50		7
	[MYT99] CB 37 2	06 00 47.6	+31 40 48		11
CB 39	IRAS 05591-1630 <sup>f</sup>	06 01 59.5	+16 30 56	outf	21
	CS peak	06 01 59.6	+16 31 44		5
	[YMT96] CB 39 2	06 02 04.6	+16 30 06		6
CB 40	IRAS 05589+1638	06 01 53.1	+16 38 35		
	IRAS 05592+1640	06 02 07.2	+16 40 11		
CB 42	IRAS 06000+1644	06 02 55.7	+16 44 36		
CB 43	[MYT99] CB 43 1	06 03 10.6	+16 36 07		11
CB 44	CS peak	06 07 29.3	+19 27 53		5
	[MYT99] CB 44 2	06 07 37.2	+19 25 12		11
	[MYT99] CB 44 3	06 07 37.6	+19 28 35		11
	IRAS 06047+1923	06 07 39.2	+19 22 43		
	IRAS 06048+1934	06 07 47.4	+19 34 18		
CB 45	IRAS 06055+1800	06 08 27.1	+17 59 59		

Table 1—Continued

Globule	Source <sup>a</sup>	Right Ascension <sup>b</sup> (J2000)	Declination <sup>b</sup> (J2000)	Included Sources <sup>c</sup>	References <sup>d</sup>
	NH <sub>3</sub> peak	06 08 56.6	+17 50 19		7
CB 48	IRAS 06175+0711	06 20 15.6	+07 10 14		
CB 50	IRAS 06316+0748	06 34 19.1	+07 45 46		
CB 51	IRAS 06355+0134	06 38 07.3	+01 31 56		
CB 52	[YMT96] CB 52 1	06 48 33.5	−16 50 31		6
	IRAS 06464-1650	06 48 39.2	−16 54 04	mm, smm	1, 2
	IRAS 06464-1644	06 48 41.8	−16 48 06		
	IRAS 06471-1651	06 49 22.2	−16 55 01		
CB 54	[YMT96] CB 54 2	07 04 21.2	−16 23 15	mm, smm, IRAS 07020-1618, outf, cs	6, 1, 2, 4, 5
CB 55	IRAS 07019-1631	07 04 12.6	−16 35 34		
CB 56	IRAS 07125-2507	07 14 36.5	−25 12 57		
	IRAS 07125-2503	07 14 38.9	−25 08 54		
CB 57	IRAS 07154-2304	07 17 32.2	−23 09 42		
	IRAS 07156-2248	07 17 45.5	−22 54 14		
	IRAS 07156-2301	07 17 47.8	−23 07 01		
CB 58	IRAS 07159-2329	07 18 02.5	−23 35 06		
	[YMT96] CB 58 1	07 18 07.6	−23 41 07		6
	IRAS 07161-2336	07 18 15.2	−23 41 42	mm, smm	1, 2
CB 59	IRAS 07171+0359	07 19 44.6	+03 53 48		
CB 60	IRAS 08022-3115	08 04 11.9	−31 24 00		
	IRAS 08026-3122	08 04 36.9	−31 30 44		
	IRAS 08029-3118	08 04 56.4	−31 27 23		
CB 63	IRAS 15486-0350	15 51 16.7	−03 59 41		
CB 65	IRAS 16277-2332	16 30 43.7	−23 39 08		
	[VRC2001] L1704 SMM 1	16 30 50.6	−23 42 08		12
	IRAS 16287-2337	16 31 44.6	−23 43 55		
CB 67	IRAS 16485-1906	16 51 10.3	−19 11 12		
CB 68	CS peak	16 57 16.3	−16 07 40		5
	IRAS 16544-1604 <sup>e</sup>	16 57 19.5	−16 09 25	mm, smm ([HSW99] CB 68 SMM 1), outf	1, 3, 13
	NH <sub>3</sub> peak	16 57 20.5	−16 09 02		7
CB 78	IRAS 17147-1821	17 17 38.5	−18 24 14		
CB 81	outflow	17 22 26.5	−27 08 10		4
CB 82	[VRC2001] L57 SMM 1	17 22 38.5	−23 49 57		12
	NH <sub>3</sub> peak	17 22 39.3	−23 49 46		14

Table 1—Continued

Globule	Source <sup>a</sup>	Right Ascension <sup>b</sup> (J2000)	Declination <sup>b</sup> (J2000)	Included Sources <sup>c</sup>	References <sup>d</sup>
	CS peak	17 22 40.7	−23 48 46		5
CB 98	CB98-mm	17 47 00.7	−20 30 29		1
CB 100	IRAS 17490-0258	17 51 38.1	−02 59 07		
	IRAS 17493-0258	17 52 00.4	−02 58 59		
CB 101	IRAS 17503-0833	17 53 05.2	−08 33 41		
	IRAS 17505-0828	17 53 14.1	−08 28 42		
CB 104	IRAS 17526-0815	17 55 21.1	−08 15 38		
	IRAS 17533-0808	17 56 03.7	−08 09 16		
CB 105	IRAS 17561-0349	17 58 44.5	−03 49 52		
CB 106	IRAS 17577-0329	18 00 25.8	−03 29 35		
	IRAS 17580-0330	18 00 41.4	−03 30 30		
	IRAS 17586-0330	18 01 18.3	−03 30 01		
CB 108	[YMT96] CB 108 1	18 03 01.9	−20 49 37		6
CB 118	IRAS 18094-1550	18 12 22.1	−15 49 13		
CB 121	IRAS 18115-0701	18 14 17.6	−07 00 51		
	IRAS 18116-0657	18 14 18.9	−06 56 44		
CB 124	IRAS 18120+0704	18 14 31.4	+07 05 13		
	IRAS 18122+0703	18 14 42.7	+07 04 44		
CB 125	NH <sub>3</sub> peak	18 15 34.7	−18 11 12		7
CB 128	IRAS 18132-0350	18 15 52.5	−03 49 40		
CB 130	CB130-mm	18 16 14.8	−02 32 47	nh3	1, 7
CB 131	CB131-smm	18 17 00.5	−18 02 04		2
CB 137	IRAS 18219-0100	18 24 30.3	−00 58 22		
CB 142	IRAS 18272-1343	18 30 02.0	−13 41 07		
CB 145	IRAS 18296-0911	18 32 21.7	−09 09 25	mm	1
CB 146	IRAS 18293-0906	18 32 08.2	−09 03 57		
	IRAS 18294-0901	18 32 11.1	−08 59 05		
	[HSW99] CB 146 SMM 2	18 32 19.4	−08 53 00		15
	[HSW99] CB 146 SMM 1	18 32 21.3	−08 51 56		15
CB 171	[YMT96] CB 171 2	19 01 33.6	−04 31 48		6
	[YMT96] CB 171 3	19 01 55.8	−04 31 11		6
CB 177	IRAS 18599+1739	19 02 07.7	+17 43 58		
CB 178	IRAS 18595+1812	19 01 44.0	+18 16 29		
	IRAS 19002+1755	19 02 28.0	+17 59 58		

Table 1—Continued

Globule	Source <sup>a</sup>	Right Ascension <sup>b</sup> (J2000)	Declination <sup>b</sup> (J2000)	Included Sources <sup>c</sup>	References <sup>d</sup>
CB 180	NH <sub>3</sub> peak	19 06 08.6	−06 52 47		7
CB 184	IRAS 19116+1623	19 13 56.4	+16 28 27		
CB 187	IRAS 19162-0135	19 18 48.7	−01 29 39		
CB 188	IRAS 19179+1129	19 20 14.9	+11 35 35	mm	1
	Outflow	19 20 16.3	+11 35 57		4
	CS peak	19 20 19.9	+11 35 57		5
	IRAS 19180+1127	19 20 21.0	+11 32 54		
CB 189	IRAS 19180+1116	19 20 22.5	+11 22 07		
	[VRC2001] L673 SMM 7	19 20 23.1	+11 22 50		12
	[VRC2001] L673 SMM 1	19 20 25.2	+11 22 17		12
	IRAS 19180+1114	19 20 25.8	+11 19 52	smm ([VRC2001] L673 SMM 2), outf	12, 15
	IRAS 19183+1123	19 20 44.0	+11 28 55		
	IRAS 19184+1118	19 20 45.6	+11 23 50		
CB 190	IRAS 19186+2325	19 20 46.3	+23 31 31		
CB 194	IRAS 19273+1433	19 29 35.7	+14 39 23		
CB 196	IRAS 19329+1213	19 35 18.0	+12 20 36		
CB 198	IRAS 19342+1213	19 36 37.8	+12 19 59		
CB 199	[ARC92] Barn 335 9	19 36 44.4	+07 36 43		17
	[ARC92] Barn 335 1	19 36 47.6	+07 32 58		17
	IRAS 19343+0727	19 36 48.8	+07 34 29		
	[ARC92] Barn 335 2	19 36 49.5	+07 35 04		17
	NH <sub>3</sub> peak	19 36 59.0	+07 34 17		19
	IRAS 19345+0727	19 37 01.0	+07 34 11	cm ([ARC92] Barn 335 4), smm ([HSW99] B 335 SMM 1), outf	17, 2, 18
	[ARC92] Barn 335 11	19 37 08.8	+07 31 41		17
	[ARC2001] HH 119 VLA 3	19 37 10.2	+07 36 50		20
	IRAS 19347+0729	19 37 10.5	+07 36 26		
	IRAS 19348+0724	19 37 17.0	+07 31 57		
CB 203	IRAS 19413+1902	19 43 33.5	+19 09 52		
CB 205	IRAS 19427+2741	19 44 45.5	+27 48 37		
	[YMT96] CB 205 1	19 45 09.5	+27 51 06		6
	[HSW99] L 810 SMM 2	19 45 21.3	+27 50 40		2
	[YMT96] CB 205 2	19 45 21.9	+27 53 40		6
	IRAS 19433+2743 <sup>h</sup>	19 45 23.9	+27 50 58	mm, smm ([HSW99] L 810 SMM 1), outf, nh3	1, 2, 21, 22
	IRAS 19433+2751	19 45 25.2	+27 58 54		

Table 1—Continued

Globule	Source <sup>a</sup>	Right Ascension <sup>b</sup> (J2000)	Declination <sup>b</sup> (J2000)	Included Sources <sup>c</sup>	References <sup>d</sup>
	[YMT96] CB 205 3	19 45 35.1	+27 54 11		6
	IRAS 19438+2757	19 45 51.2	+28 04 23		
	IRAS 19438+2737	19 45 55.5	+27 44 58		
	IRAS 19439+2748	19 45 57.8	+27 56 06		
CB 206	[YMT96] CB 206 2	19 46 30.4	+19 06 06		6
CB 207	IRAS 19437+2108	19 45 53.0	+21 16 15		
CB 208	IRAS 19450+1847	19 47 14.7	+18 55 10		
CB 210	IRAS 19529+3341	19 54 49.1	+33 49 15		
CB 211	IRAS 19576+2447	19 59 46.5	+24 55 35		
CB 214	IRAS 20018+2629	20 03 57.9	+26 38 20	outf	4, 21
CB 216	Outflow	20 05 49.7	+23 27 04		4
	IRAS 20037+2317	20 05 53.6	+23 26 34	cs	5
	CS peak	20 05 54.1	+23 26 16	IRAS 20037+2317	5
CB 217	Outflow	20 07 45.9	+37 07 01		21
	[YMT96] CB 217 4	20 07 51.5	+37 06 55		6
CB 219	IRAS 20176+6343	20 18 23.7	+63 52 30		
CB 222	IRAS 20328+6351	20 33 36.4	+64 02 21		
CB 224	NH <sub>3</sub> peak	20 36 20.3	+63 52 55		7
	IRAS 20355+6343	20 36 22.1	+63 53 39	mm	1
CB 225	IRAS 20365+5607	20 37 48.0	+56 17 56		
CB 230	[YMT96] CB 230 1	21 17 30.9	+68 18 10		
	[YMT96] CB 230 2	21 17 38.5	+68 17 32	mm, smm ([HSW99] CB 230 SMM 1), IRAS 21169+6804, outf, cs	6, 1, 2, 15, 4, 21, 5
CB 232	IRAS 21352+4307	21 37 11.3	+43 20 36	smm ([HSW99] CB 232 SMM 1, [HSW99] CB 232 SMM 2), outf, cs	15, 4, 5
CB 233	CS peak	21 40 26.4	+57 48 06		5
CB 235	IRAS 21548+5843	21 56 25.7	+58 57 54		
CB 238	NH <sub>3</sub> peak	22 13 22.6	+41 02 51		7
CB 240	IRAS 22317+5816	22 33 39.3	+58 31 56	mm	1
CB 241	IRAS 23095+6547	23 11 37.0	+66 04 07		
CB 243	IRAS 23228+6320	23 25 05.7	+63 36 34	mm, smm ([VRC2001] L1246 SMM 1), nh3	1, 23, 12, 7
	NH <sub>3</sub> peak	23 25 06.9	+63 36 50	smm ([VRC2001] L1246 SMM 1), IRAS 23228+6320	7, 23, 12
	[VRC2001] L1246 SMM 2	23 25 16.4	+63 36 46		23, 12
	CS peak	23 25 27.0	+63 35 46		5
CB 244	[VRC2001] L1262 SMM 2	23 25 26.0	+74 18 28	nh3	12, 23, 24
	[YMT96] CB 244 1	23 25 46.6	+74 17 40	mm, smm ([VRC2002] L1262 SMM 1), IRAS 23238+7401, outf	6, 1, 2, 12, 4

Table 1—Continued

Globule	Source <sup>a</sup>	Right Ascension <sup>b</sup> (J2000)	Declination <sup>b</sup> (J2000)	Included Sources <sup>c</sup>	References <sup>d</sup>
	IRAS 23249+7406	23 26 53.2	+74 22 34		
CB 246	CB246-mm	23 56 43.6	+58 34 29		1
CB 247	IRAS 23550+6430	23 57 36.4	+64 46 48		

<sup>a</sup>Target sources. SIMBAD names were used, where available. Labels [YMT96], [MYT99], [ARC92], and [ARC2001] indicate cm sources

<sup>b</sup>Coordinates of pointing position. Units of right ascension are hours, minutes, and seconds. Units of declination are degrees, arcminutes, and arcseconds

<sup>c</sup>Other sources included within the telescope beam, complying any of the selection criteria mentioned in sec. 3. Cm: centimeter source; mm: millimeter source; smm: submillimeter source; outf: center of molecular outflow; nh3: peak of NH<sub>3</sub> map; cs: peak of CS map. Where available, SIMBAD names are given between parentheses

<sup>d</sup>References for the sources complying the selection criteria (except for IRAS sources)

<sup>e</sup>Maser detected by Scappini et al. (1991)

<sup>f</sup>Maser detected by Schwartz & Buhl (1975)

<sup>g</sup>Coordinates used for IRAS 16544-1604 are those in the IRAS Point Source Catalog. SIMBAD reports for this source the coordinates of F16544-1604 in the IRAS Faint Source Catalog, which is also within the Robledo beam from our pointing position

<sup>h</sup>Maser detected by Neckel et al. (1985)

References. — (1) Launhardt & Henning (1997); (2) Launhardt et al. (1997); (3) Huard et al. (2000); (4) Yun & Clemens (1992); (5) Launhardt et al. (1998); (6) Yun et al. (1996); (7) Lemme et al. (1996); (8) Harvey et al. (2002); (9) Moreira et al. (1999); (10) Codella & Scappini (1998); (11) Moreira et al. (1999); (12) Visser et al. (2002); (13) Vallée, Bastien, & Greaves (2000); (14) Bourke et al. (1995b); (15) Huard et al. (1999); (16) Armstrong & Winnewisser (1989); (17) Anglada et al. (1992); (18) Frerking & Langer (1982); (19) Benson & Myers (1989); (20) Avila, Rodríguez, & Curiel (2001); (21) Yun & Clemens (1994a); (22) Neckel et al. (1985); (23) Visser et al. (2001); (24) Benson, Myers, & Wright (1984)

Table 2. Water maser detections

Globule	Source	$S_\nu^a$ (Jy)	$\int S_\nu dV^b$ (Jy km s $^{-1}$ )	$V_{\text{peak}}^c$ (km s $^{-1}$ )	$V_{\text{cloud}}^d$ (km s $^{-1}$ )	Date $^e$
CB 3	CB3-mm	$11.0 \pm 0.4$	$52 \pm 3$	$-53.4 \pm 0.6$	$-38.3$	2004-JUL-24
		$12.4 \pm 0.4$	$80.2 \pm 2.4$	$-53.5 \pm 0.6$		2004-AUG-19
		$19.60 \pm 0.22$	$97 \pm 3$	$-41.1 \pm 0.6$		2005-JAN-03
		$12.00 \pm 0.13$	$56.0 \pm 0.7$	$-41.8 \pm 0.6$		2005-JAN-31
CB 34	[HSW99] CB 34 SMM 3	$0.34 \pm 0.08$	$0.57 \pm 0.23$	$8.1 \pm 0.6$	$0.7$	2004-AUG-20
		$0.33 \pm 0.07$	$0.57 \pm 0.20$	$8.1 \pm 0.6$		2004-AUG-25
		$< 0.14$				2005-APR-14
		$< 0.14$				2005-APR-18
CB 54	[YMT96] CB 54 2	$0.84 \pm 0.22$	$1.1 \pm 0.5$	$13.7 \pm 0.5$	$19.5$	2002-MAY-26
		$0.88 \pm 0.20$	$0.7 \pm 0.3$	$7.9 \pm 0.5$		2003-MAY-04
		$14.1 \pm 0.4$	$12.6 \pm 0.7$	$7.9 \pm 0.5$		2003-JUN-07
		$49.3 \pm 0.9$	$45.3 \pm 1.8$	$7.9 \pm 0.5$		2003-JUN-29
		$41.1 \pm 0.5$	$39.9 \pm 0.9$	$7.9 \pm 0.5$		2003-JUL-01
		$5.24 \pm 0.11$	$9.5 \pm 0.4$	$8.7 \pm 0.6$		2005-APR-02
CB 65	IRAS 16277-2332	$0.30 \pm 0.19$	$0.6 \pm 0.3$	$1.2 \pm 0.5$	$2.3$	2002-JUN-16
		$< 0.25$				2004-JUL-08
		$< 0.18$				2004-JUL-14
		$< 0.22$				2005-JUN-05
CB 101	IRAS 17503-0833	$0.26 \pm 0.05$	$0.41 \pm 0.13$	$29.3 \pm 1.3$	$6.7$	2002-APR-10
		$0.32 \pm 0.09$	$0.41 \pm 0.15$	$28.3 \pm 0.5$		2002-APR-14
		$0.55 \pm 0.19$	$0.63 \pm 0.25$	$29.3 \pm 0.5$		2002-NOV-15
		$0.60 \pm 0.15$	$0.52 \pm 0.21$	$28.9 \pm 0.6$		2004-JUL-07
		$0.34 \pm 0.17$	$0.6 \pm 0.4$	$28.9 \pm 0.6$		2004-JUL-14
		$0.58 \pm 0.18$	$0.6 \pm 0.3$	$29.0 \pm 0.6$		2004-AUG-04
CB 199	[ARC2001] HH 119 VLA 3	$0.49 \pm 0.06$	$0.69 \pm 0.15$	$37.9 \pm 0.6$	$8.4$	2005-JUN-16
		$0.36 \pm 0.10$	$0.41 \pm 0.18$	$37.8 \pm 0.6$		2005-JUL-21
CB 232	IRAS 21352+4307	$0.34 \pm 0.10$	$0.46 \pm 0.19$	$12.1 \pm 0.5$	$12.6$	2003-MAY-10
		$0.82 \pm 0.13$	$1.10 \pm 0.23$	$12.1 \pm 0.5$		2003-MAY-11
		$0.62 \pm 0.19$	$0.51 \pm 0.24$	$10.5 \pm 0.5$		2003-JUL-15
		$0.94 \pm 0.12$	$0.95 \pm 0.23$	$9.4 \pm 0.6$		2005-APR-02

<sup>a</sup>Flux density of the strongest maser feature. Uncertainties are  $2\sigma$ .

<sup>b</sup>Flux density integrated over the velocity extent of the maser emission. Uncertainties are  $2\sigma$ .

<sup>c</sup>SR Velocity of the strongest maser feature

<sup>d</sup>SR Velocity of the globule, as given in the CB catalog

<sup>e</sup>Date of observation

Table 3. Non detections

Globule	Source	$V_{\min}^a$ (km s <sup>-1</sup> )	$V_{\max}^a$ (km s <sup>-1</sup> )	Rms <sup>b</sup> (Jy)	Date <sup>c</sup>
CB 3	[YMT96] CB 3 1	-2696	2698	0.03	2002-APR-09
		-139.4	62.8	0.14	2002-OCT-13
CB 4	IRAS 00362+5234	-112.4	89.8	0.05	2003-MAY-10
CB 6	IRAS 00465+6028	-113.6	88.6	0.06	2003-MAY-10
CB 7	IRAS 01078+6409	-107.8	107.9	0.06	2004-AUG-04
	IRAS 01087+6404	-107.8	107.9	0.08	2004-AUG-04
		-107.7	108.0	0.04	2005-APR-14
CB 8	IRAS 01202+7406	-105.7	110.0	0.05	2004-AUG-04
CB 11	IRAS 01333+6448	-109.8	105.9	0.07	2004-AUG-04
	IRAS 01334+6442	-109.8	106.0	0.05	2004-AUG-04
	IRAS 01341+6447	-109.7	106.0	0.06	2004-AUG-05
CB 12	CS peak	-112.5	89.7	0.09	2003-MAY-09
		-119.4	96.4	0.05	2004-JUL-09
	IRAS 01354+6447	-119.3	96.4	0.05	2004-AUG-20
CB 15	IRAS 03521+5555	-107.2	108.5	0.08	2004-AUG-19
	IRAS 03523+5608	-107.2	108.5	0.10	2004-AUG-19
		-107.1	108.7	0.07	2005-APR-14
	IRAS 03535+5555	-107.2	108.5	0.05	2004-AUG-20
CB 16	IRAS 03592-5642	-2716	2677	0.05	2002-APR-09
		-103.3	98.9	0.10	2002-NOV-15
CB 17	IRAS 04005+5647	-112.8	103.0	0.05	2004-JUL-27
	NH <sub>3</sub> peak	-105.8	96.4	0.05	2003-MAY-09
CB 19	IRAS 04233+2529	-101.5	114.2	0.04	2004-AUG-20
	IRAS 04240+2535	-101.5	114.2	0.04	2004-AUG-20
CB 22	NH <sub>3</sub> peak	-105.6	110.1	0.05	2004-AUG-20
CB 23	NH <sub>3</sub> peak	-105.8	109.9	0.05	2004-AUG-20
	CB23-cm1	-102.6	113.1	0.06	2004-JUL-15
		-102.1	113.7	0.05	2005-APR-14
	CB23-cm2	-102.5	113.2	0.05	2004-JUL-27
CB 26	IRAS 04559+5200	-2722	2671	0.07	2002-APR-09

Table 3—Continued

Globule	Source	$V_{\min}^a$ (km s <sup>-1</sup> )	$V_{\max}^a$ (km s <sup>-1</sup> )	Rms <sup>b</sup> (Jy)	Date <sup>c</sup>
CB 27	IRAS 05013+3234	-101.2	114.6	0.08	2004-SEP-04
CB 28	IRAS 05036-0359	-99.2	116.5	0.10	2004-SEP-08
	IRAS 05037-0402	-99.3	116.5	0.12	2004-SEP-08
	CS peak	-92.3	109.9	0.3	2002-NOV-17
		-92.3	109.9	0.07	2003-MAY-10
	IRAS 05038-0400	-99.3	116.5	0.07	2004-SEP-08
	NH <sub>3</sub> peak	-92.3	109.9	0.4	2002-NOV-17
		-92.3	109.9	0.11	2003-MAY-09
CB 29	IRAS 05190-0348	-96.8	119.0	0.06	2004-OCT-05
		-96.7	119.1	0.04	2004-OCT-31
	IRAS 05194-0346	-96.8	119.0	0.06	2004-SEP-08
	IRAS 05194-0343	-96.7	119.0	0.06	2004-OCT-05
		-96.7	119.0	0.05	2004-OCT-31
	CS peak	-89.9	112.3	0.4	2002-NOV-17
		-89.9	112.3	0.08	2003-MAY-10
		-96.6	119.1	0.04	2005-APR-14
	IRAS 05201-0341	-96.6	119.1	0.04	2004-OCT-31
CB 30	[MYT99] CB 30 3	-101.2	101.0	0.08	2003-MAY-11
	IRAS 05274+0542	-108.2	107.6	0.06	2004-OCT-05
		-108.1	107.6	0.05	2004-OCT-30
	IRAS 05268+0538	-101.2	101.0	0.11	2003-MAY-08
	IRAS 05268+0550	-108.1	107.6	0.05	2004-OCT-05
		-108.1	107.6	0.05	2004-OCT-29
CB 31	[YMT96] CB 31 1	-108.3	93.9	0.10	2003-MAY-08
	[YMT96] CB 31 2	-108.3	93.9	0.08	2003-MAY-06
	IRAS 05307-0038	-115.0	100.7	0.06	2004-OCT-05
		-115.0	100.8	0.07	2004-OCT-07
		-104.2	111.5	0.04	2004-OCT-26
CB 32	IRAS 05344-0016	-112.9	102.8	0.06	2004-OCT-31
	CS peak	-106.2	96.0	0.14	2003-MAY-09

Table 3—Continued

Globule	Source	$V_{\min}^a$ (km s <sup>-1</sup> )	$V_{\max}^a$ (km s <sup>-1</sup> )	Rms <sup>b</sup> (Jy)	Date <sup>c</sup>
		-106.2	96.0	0.12	2003-MAY-10
CB 33	IRAS 05433+2040	-107.3	108.4	0.10	2004-SEP-04
	IRAS 05437+2045	-107.3	108.4	0.09	2004-SEP-04
CB 34	[HSW99] CB 34 SMM 2	-107.4	108.3	0.05	2004-AUG-20
	[YMT96] CB 34 3	-100.4	101.8	0.05	2003-MAY-06
	[HSW99] CB 34 SMM 1	-93.9	121.8	0.06	2004-JUL-27
	[HSW99] CB 34 SMM 5	-107.4	108.3	0.06	2005-SEP-23
CB 37	[MYT99] CB 37 1	-99.9	102.3	0.10	2003-JUL-15
		-107.0	108.7	0.07	2004-AUG-27
		-104.4	111.4	0.04	2005-APR-14
	NH <sub>3</sub> peak	-107.0	108.8	0.05	2004-AUG-20
	[MYT99] CB 37 2	-107.0	108.7	0.05	2004-AUG-20
CB 39	IRAS 05591-1630	-98.7	103.5	0.07	2003-MAY-10
	CS peak	-98.7	103.5	0.14	2003-MAY-08
	[YMT96] CB 39 2	-98.7	103.5	0.05	2003-MAY-06
CB 40	IRAS 05589+1638	-118.9	96.9	0.07	2004-SEP-05
	IRAS 05592+1640	-105.4	110.3	0.10	2004-SEP-05
CB 42	IRAS 06000+1644	-105.2	110.6	0.08	2004-OCT-07
		-105.1	110.7	0.06	2004-OCT-26
CB 43	[MYT99] CB 43 1	-101.6	114.2	0.04	2005-OCT-16
CB 44	CS peak	-101.6	100.6	0.06	2003-MAY-07
	[MYT99] CB 44 2	-101.6	100.6	0.06	2003-MAY-11
	[MYT99] CB 44 3	-101.6	100.6	0.07	2003-MAY-11
	IRAS 06047+1923	-108.6	107.2	0.06	2004-OCT-07
		-108.3	107.4	0.10	2004-OCT-26
	IRAS 06048+1934	-101.6	100.6	0.23	2003-MAY-08
CB 45	IRAS 06055+1800	-107.2	108.5	0.07	2004-OCT-07
		-107.2	108.5	0.05	2004-OCT-30
	NH <sub>3</sub> peak	-100.3	101.9	0.10	2003-MAY-07
CB 48	IRAS 06175+0711	-89.4	126.3	0.04	2004-OCT-30

Table 3—Continued

Globule	Source	$V_{\min}^a$ (km s <sup>-1</sup> )	$V_{\max}^a$ (km s <sup>-1</sup> )	Rms <sup>b</sup> (Jy)	Date <sup>c</sup>
CB 50	IRAS 06316+0748	-107.1	108.6	0.04	2004-OCT-30
CB 51	IRAS 06355+0134	-117.2	98.5	0.06	2004-DEC-01
CB 52	[YMT96] CB 52 1	-91.4	124.3	0.06	2004-OCT-30
	IRAS 06464-1650	-85.6	116.6	0.10	2003-MAY-07
	IRAS 06464-1644	-91.4	124.4	0.04	2005-FEB-19
	IRAS 06471-1651	-91.3	124.5	0.04	2005-FEB-19
CB 55	IRAS 07019-1631	-87.8	127.8	0.03	2005-FEB-19
CB 56	IRAS 07125-2507	-93.3	122.4	0.04	2005-FEB-19
	IRAS 07125-2503	-93.3	122.4	0.04	2005-FEB-19
CB 57	IRAS 07154-2304	-87.6	128.1	0.08	2005-FEB-22
	IRAS 07156-2248	-87.4	128.3	0.21	2004-DEC-01
	IRAS 07156-2301	-87.4	128.4	0.06	2005-FEB-19
CB 58	IRAS 07159-2329	-87.4	128.3	0.07	2005-FEB-22
	[YMT96] CB 58 1	-85.6	116.6	0.18	2003-MAY-04
	IRAS 07161-2336	-85.6	116.6	0.10	2003-MAY-07
CB 59	IRAS 07171+0359	-90.5	111.7	0.05	2002-APR-18
CB 60	IRAS 08022-3115	-93.9	121.8	0.07	2005-FEB-19
	IRAS 08026-3122	-94.0	121.8	0.23	2004-DEC-01
	IRAS 08029-3118	-93.0	121.8	0.11	2004-DEC-30
CB 63	IRAS 15486-0350	-2665	2728	0.02	2002-APR-09
CB 65	[VRC2001] L1704 SMM 1	-132.6	83.1	0.09	2004-AUG-04
	IRAS 16287-2337	-98.8	103.4	0.16	2002-JUN-16
CB 67	IRAS 16485-1906	-130.3	85.4	0.08	2004-AUG-04
CB 68	CS peak	-102.6	113.1	0.08	2004-JUL-09
		-102.7	113.0	0.05	2005-JUN-06
	IRAS 16544-1604	-102.7	113.0	0.05	2004-JUL-08
	NH <sub>3</sub> peak	-102.8	113.0	0.10	2004-AUG-21
CB 78	IRAS 17147-1821	-2720	2673	0.06	2002-MAR-13
CB 81	outflow	-104.3	111.4	0.15	2004-JUL-04
CB 82	[VRC2001] L57 SMM 1	-104.2	111.5	0.3	2004-JUL-23

Table 3—Continued

Globule	Source	$V_{\min}^a$ (km s <sup>-1</sup> )	$V_{\max}^a$ (km s <sup>-1</sup> )	Rms <sup>b</sup> (Jy)	Date <sup>c</sup>
		-101.0	114.7	0.06	2005-JUN-06
	NH <sub>3</sub> peak	-104.4	111.3	0.12	2004-AUG-26
	CS peak	-97.5	104.7	0.06	2004-JUL-08
CB 98	CB98-mm	-97.0	118.7	0.14	2004-JUL-23
CB 100	IRAS 17490-0258	-96.5	105.7	0.10	2002-NOV-16
	IRAS 17493-0258	-103.1	112.7	0.05	2004-AUG-21
CB 101	IRAS 17505-0828	-2654	2739	0.02	2002-APR-10
		-101.1	114.6	0.07	2004-AUG-04
CB 104	IRAS 17526-0815	-2654	2738	0.03	2002-APR-10
	IRAS 17533-0808	-97.1	118.6	0.05	2004-AUG-21
CB 105	IRAS 17561-0349	-100.9	114.8	0.09	2004-AUG-21
CB 106	IRAS 17577-0329	-91.5	124.2	0.06	2004-JUL-15
	IRAS 17580-0330	-101.5	114.2	0.05	2004-AUG-26
	IRAS 17586-0330	-101.5	114.3	0.06	2004-AUG-26
CB 108	[YMT96] CB 108 1	-95.5	106.7	0.3	2002-SEP-30
		-102.1	113.6	0.05	2005-JUN-06
CB 118	IRAS 18094-1550	-2654	2739	0.03	2002-APR-08
CB 121	IRAS 18115-0701	-101.9	113.9	0.08	2004-AUG-21
	IRAS 18116-0657	-101.9	113.8	0.09	2004-AUG-26
CB 124	IRAS 18120+0704	-87.2	128.5	0.05	2004-JUL-15
	IRAS 18122+0703	-80.7	121.5	0.20	2002-NOV-15
CB 125	NH <sub>3</sub> peak	-94.7	107.5	0.8	2002-OCT-02
CB 128	IRAS 18132-0350	-99.0	116.7	0.06	2004-JUL-07
CB 130	CB130-mm	-97.6	118.1	0.06	2004-JUL-22
CB 131	CB131-smm	-101.0	114.7	0.10	2004-JUL-24
CB 137	IRAS 18219-0100	-98.4	117.3	0.10	2004-AUG-04
CB 142	IRAS 18272-1343	-89.1	126.6	0.06	2004-JUL-08
CB 145	IRAS 18296-0911	-103.1	112.7	0.05	2004-JUL-07
CB 146	IRAS 18293-0906	-103.3	112.4	0.06	2004-JUL-09
	IRAS 18294-0901	-103.3	112.5	0.07	2004-JUL-09

Table 3—Continued

Globule	Source	$V_{\min}^a$ (km s <sup>-1</sup> )	$V_{\max}^a$ (km s <sup>-1</sup> )	Rms <sup>b</sup> (Jy)	Date <sup>c</sup>
	[HSW99] CB 146 SMM 2	-103.3	112.4	0.05	2004-JUL-08
	[HSW99] CB 146 SMM 1	-103.3	112.4	0.05	2004-JUL-08
CB 171	[YMT96] CB 171 3	-90.9	124.9	0.05	2004-JUL-22
	[YMT96] CB 171 2	-90.9	124.8	0.06	2004-JUL-22
CB 177	IRAS 18599+1739	-91.2	124.5	0.08	2004-SEP-04
CB 178	IRAS 18595+1812	-92.2	123.5	0.13	2004-SEP-05
	IRAS 19002+1755	-92.2	123.5	0.07	2004-AUG-27
CB 180	NH <sub>3</sub> peak	-95.9	119.9	0.04	2004-JUL-09
CB 184	IRAS 19116+1623	-2655	2738	0.03	2002-APR-08
CB 187	IRAS 19162-0135	-101.2	114.5	0.10	2004-SEP-03
CB 188	IRAS 19179+1129	-99.9	115.8	0.07	2004-AUG-25
	Outflow	-100.4	115.3	0.07	2004-JUL-09
	CS peak	-94.0	108.2	0.10	2002-SEP-18
	IRAS 19180+1127	-100.4	115.3	0.05	2004-JUL-09
CB 189	IRAS 19180+1116	-99.9	115.8	0.08	2004-AUG-25
	[VRC2002] L673 SMM 7	-100.1	115.6	0.04	2005-JUN-06
	[VRC2002] L673 SMM 1	-100.0	115.7	0.07	2005-FEB-26
		-100.8	115.0	0.05	2005-JUN-16
	IRAS 19180+1114	-100.0	115.8	0.05	2005-SEP-22
	IRAS 19183+1123	-100.4	115.3	0.06	2004-AUG-22
	IRAS 19184+1118	-100.5	115.3	0.06	2004-AUG-22
CB 190	IRAS 19186+2325	-96.5	119.3	0.09	2004-AUG-22
CB 194	IRAS 19273+1433	-103.7	112.1	0.12	2004-SEP-10
CB 196	IRAS 19329+1213	-97.7	118.0	0.10	2004-SEP-09
CB 198	IRAS 19342+1213	-97.7	118.0	0.06	2004-OCT-25
		-99.0	116.7	0.05	2005-JUN-16
CB 199	[ARC92] Barn 335 9	-99.2	116.5	0.09	2005-FEB-27
	[ARC92] Barn 335 1	-108.9	106.8	0.05	2004-NOV-09
	IRAS 19343+0727	-99.2	116.5	0.08	2004-AUG-18
	[ARC92] Barn 335 2	-108.9	106.8	0.06	2004-NOV-09

Table 3—Continued

Globule	Source	$V_{\min}^a$ (km s <sup>-1</sup> )	$V_{\max}^a$ (km s <sup>-1</sup> )	Rms <sup>b</sup> (Jy)	Date <sup>c</sup>
		-99.2	116.5	0.10	2005-FEB-22
	NH <sub>3</sub> peak	-99.2	116.5	0.06	2004-AUG-18
		-99.2	116.5	0.12	2005-FEB-22
		-99.3	116.4	0.05	2005-JUN-16
	IRAS 19345+0727	-92.7	109.5	0.13	2003-MAY-16
	[ARC92] Barn 335 11	-99.6	116.1	0.05	2005-JUN-15
	IRAS 19347+0729	-99.1	116.6	0.07	2004-SEP-03
	IRAS 19348+0724	-99.1	116.6	0.07	2004-SEP-04
CB 203	IRAS 19413+1902	-91.7	124.1	0.09	2004-SEP-04
CB 205	IRAS 19427+2741	-93.6	122.1	0.07	2004-AUG-22
		-85.1	117.2	0.06	2005-JUN-16
	[YMT96] CB 205 1	-85.3	116.9	0.07	2002-SEP-03
		-85.3	116.9	0.10	2002-SEP-19
		-85.3	116.9	0.13	2002-NOV-16
	[HSW99] L 810 SMM 2	-91.7	124.0	0.05	2004-JUL-22
	[YMT96] CB 205 2	-2659	2734	0.03	2002-APR-08
	IRAS 19433+2743	-85.3	116.9	0.25	2003-JUL-11
		-91.7	124.0	0.05	2004-JUL-22
		-91.8	124.0	0.05	2005-JUN-16
	IRAS 19433+2751	-91.7	124.1	0.07	2004-AUG-25
	[YMT96] CB 205 3	-85.3	116.9	0.08	2002-SEP-03
		-85.3	116.9	0.17	2002-NOV-16
		-91.7	124.0	0.05	2004-JUL-15
	IRAS 19438+2757	-91.6	124.1	0.07	2004-AUG-25
	IRAS 19438+2737	-91.7	124.0	0.10	2004-AUG-25
	IRAS 19439+2748	-91.7	124.1	0.07	2004-SEP-05
CB 206	[YMT96] CB 206 2	-92.2	123.5	0.07	2004-JUL-22
		-92.3	123.4	0.05	2004-AUG-05
CB 207	IRAS 19437+2108	-99.9	115.9	0.06	2004-AUG-05
CB 208	IRAS 19450+1847	-92.1	123.6	0.11	2004-SEP-10

Table 3—Continued

Globule	Source	$V_{\min}^a$ (km s <sup>-1</sup> )	$V_{\max}^a$ (km s <sup>-1</sup> )	Rms <sup>b</sup> (Jy)	Date <sup>c</sup>
CB 210	IRAS 19529+3341	-97.8	118.0	0.09	2004-SEP-04
CB 211	IRAS 19576+2447	-100.5	115.2	0.10	2004-SEP-04
CB 214	IRAS 20018+2629	-91.2	111.0	0.14	2003-JUL-11
CB 216	Outflow	-88.5	113.7	0.14	2002-SEP-17
	IRAS 20037+2317	-94.8	120.9	0.10	2004-SEP-05
	CS peak	-2659	2734	0.03	2002-APR-08
		-88.5	113.7	0.13	2002-SEP-17
CB 217	Outflow	-100.6	101.6	0.12	2003-JUL-11
	[YMT96] CB 217 4	-107.0	108.7	0.06	2004-JUL-24
CB 219	IRAS 20176+6343	-2680	2713	0.03	2002-APR-08
CB 222	IRAS 20328+6351	-101.0	101.2	0.04	2002-APR-19
CB 224	IRAS 20355+6343	-103.8	98.4	0.19	2003-JUN-07
		-110.3	105.3	0.04	2004-OCT-29
		-110.7	105.0	0.04	2005-JUN-05
		-2681	2713	0.04	2003-APR-08
CB 225	IRAS 20365+5607	-103.6	98.6	0.06	2002-APR-18
		-103.6	98.6	0.13	2002-AUG-14
CB 230	[YMT96] CB 230 1	-98.2	104.0	0.04	2002-APR-19
	[YMT96] CB 230 2	-2685	2708	0.05	2002-APR-07
CB 233	CS peak	-108.5	107.3	0.10	2004-AUG-19
		-109.3	106.4	0.05	2005-APR-14
CB 235	IRAS 21548+5843	-108.0	107.8	0.10	2004-AUG-19
CB 238	NH <sub>3</sub> peak	-107.3	108.4	0.05	2004-AUG-22
CB 240	IRAS 22317+5816	-111.5	104.3	0.08	2004-JUL-30
CB 241	IRAS 23095+6547	-115.5	100.3	0.08	2004-JUL-30
CB 243	IRAS 23228+6320	-112.2	90.0	0.09	2003-MAY-11
	NH <sub>3</sub> peak	-112.2	90.0	0.20	2002-OCT-13
	[VRC2001] L1246 SMM 2	-119.0	96.8	0.07	2004-JUL-24
	CS peak	-119.0	96.8	0.06	2004-JUL-24
CB 244	[VRC2001] L1262 SMM 2	-104.0	111.8	0.08	2004-JUL-30

Table 3—Continued

Globule	Source	$V_{\min}^a$ (km s <sup>-1</sup> )	$V_{\max}^a$ (km s <sup>-1</sup> )	Rms <sup>b</sup> (Jy)	Date <sup>c</sup>
	[YMT96] CB 244 1	-2694	2699	0.04	2002-APR-07
	IRAS 23249+7406	-97.2	105.0	0.12	2003-JUN-07
CB 246	CB246-mm	-103.6	112.2	0.08	2004-JUL-24
CB 247	IRAS 23550+6430	-104.8	97.4	0.06	2003-MAY-12

<sup>a</sup>Velocity range covered by the observational bandwidth

<sup>b</sup>Noise level,  $1\sigma$

<sup>c</sup>Date of observation